4 JULY 2023

FUNCTIONAL ULTRASOUND ASSESSMENT OF EXTERNAL ANAL SPHINCTER IN HEALTHY WOMEN AND PATIENTS WITH PREVIOUS OBSTETRIC ANAL SPHINCTER INJURY

GRADUATION THESIS – TECHNICAL MEDICINE

UNIVERSITY OF TWENTE.

DIONNE NIJLAND

SUPERVISION

Chair:	Prof. Dr. R.H. Geelkerken
Technological supervisor:	Dr. A.T.M. Bellos-Grob
Medical supervisors:	Dr. A.L. Veenstra van Nieuwenhoven
	Drs. K.S. Dekker
Process supervisor:	Drs. A.G. Lovink
External member:	Dr. J.M. Wolterink

Table of contents

Abstract 2
1. Introduction 3
2. Materials and methods 5
2.1. Study population 5
2.2. Data acquisition/collection 5
2.3. Data processing 7
2.4. Data analysis displacements 10
3. Results 11
3.1. Segmentation 12
3.2. Orientation sphincter 13
3.3. Displacement controls 14
3.4. Displacement OASI 16
3.5. Comparison control and patient 18
4. Discussion 19
4.1. EAS segmentation 19
4.2. Displacements 19
4.3. Drawback analysis 20
4.4. Future perspectives 21
5. Conclusion 22
References 22
Appendices 24
Appendix A: Anatomical background information of the EAS 24
Appendix B: Segmentation results of the controls 26
Appendix C: Segmentation results of the patients 31
Appendix D: Displacement figures of the controls 36
Appendix E: Displacement figures of the patients 41

Abstract

Introduction: About 3.5% of women experience an obstetric anal sphincter injury (OASI) at first delivery, damaging the external anal sphincter (EAS). It is still unclear whether women can give birth vaginally in a new pregnancy (with good sphincter repair) or whether a caesarean section is advised to avoid further damaging a weak sphincter. The current ZGT guideline includes symptoms and ultrasound-determined anatomic damage but not EAS function. This study aims to use functional 4D ultrasound to determine the difference in the displacement of the EAS during contraction between women with and without an OASI.

Method: In five nullipara women (controls) and five women with a previous OASI (patients), a 4D transperineal ultrasound recording (3D + time) was made of the EAS. Recordings were made from rest to maximal contraction. The EAS was segmented in the rest frame and tracked to maximum contraction. The displacement of the EAS was calculated per voxel in 3 directions (caudal/cranial, anterior/posterior and left/right). These displacements were compared between the control and patient groups.

Results: In the caudal/cranial direction, we observe a similar displacement of the EAS between the groups. In the anterior/posterior direction, in the control group, the displacement is highest on the left and right side of the EAS, while in the patient group, this mostly happens only on one side. In addition, in the left/right direction of the control group, the left and right parts are closing, while in the patient group, these parts open.

Conclusion: There is a difference in the displacement of the EAS measured by 4D ultrasound between healthy women and women with a previous obstetric anal sphincter injury. These differences support our hypothesis that there are functional differences between the groups and that through transperineal ultrasound, these should be included in the care around OASI.

1. Introduction

Vaginal delivery is the main risk factor for pelvic floor disorders (PFD) [1], such as pelvic organ prolapse, urinary incontinence, and faecal incontinence (FI). Especially FI has a high negative impact on the quality of life and can be divided into the loss of gasses, fluid and/or feces[2]. FI can be prevented by an adequately coordinated function of three (intact) pelvic floor muscles, namely the puborectalis muscle (PRM), internal anal sphincter (IAS) and external anal sphincter (EAS)[3]. The PRM forms a sling around the anal canal and relaxes during defecation to create a straight passage for the feces. The passage space will decrease during PRM contraction and can be consciously contracted. The IAS is an involuntary muscle contracted at rest and relaxes with an increase in rectum filling, which allows defecation of the rectum [3]. The EAS is a voluntary muscle that automatically contracts more due to higher abdominal pressure or increased rectum filling without the urgency to defecate. It is also possible to contract the EAS consciously at moments of urgency, and when defecation is not preferred, so the EAS prevents the unintended loss of feces [3].

FI can be caused by various aspects such as age, chronic diarrhea, neurologic diseases, or sphincter trauma[4], [5]. However, an essential factor for FI in women is an obstetric anal sphincter injury (OASI) [6]–[8]. The severity of OASI can be classified with the Sultan classification into grades 1 to 4 [9]. The EAS is ruptured in case of more severe OASI (grades 3 and 4). Figure 1 illustrates a schematic representation of the OASI grades 3 to 4. In grade 3a, up to 50% of the external anal sphincter (EAS) is ruptured. In grade 3b, 50% up to 100% of the EAS is ruptured while the internal anal sphincter (IAS) is intact. In grade 3c, the internal anal sphincter is involved as well. Grade 4 is the most severe OASI, and the tear completely extends into the anal sphincter, including the rectal mucosal surface [10], [11]. In 2020 in the Netherlands, an OASI grade 3 or 4 occurred in 3.55% of the first (nulliparous) deliveries after 37 weeks of gestation and occurred in 1.36% of multiparous women [12]. The study of Nilsson et al. [13] shows comparable results for nulliparous and multiparous women, 3.9% and between 0.7 and 1.1%, respectively. The risk of a repeated OASI was 10-fold of the change for multiparous women without previous OASI [13]. The prevalence of women with FI after two singleton vaginal deliveries doubled to 23.7% for 1 OASI and tripled to 36.1% for 2 OASIs, compared to 11.7% for women without OASI [13].

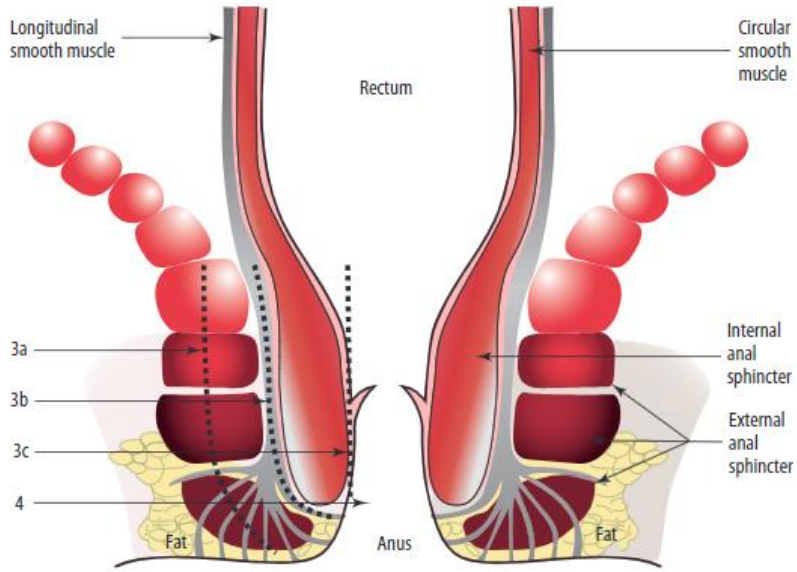

Figure 1. Classification of OASI grade 3 to 4 in a schematic representation of the anal sphincter [11]*. Grade 3a is a rupture up to the first dotted line. Grade 3b is between the first and second dotted lines. Grade 3c is between the second and third dotted line, and grade 4 is past the third dotted line.*

The current protocol in Ziekenhuisgroep Twente (ZGT) is that pregnant women with previous OASI get a 2D endoanal ultrasound (EAUS) to determine the extent of the sphincter injury [14]. The sphincter is classified with 2D EAUS as normal when less than 1/12 part of the sphincter in the transversal plane is damaged, mild when 1/12 to 3/12 part of the sphincter in the transversal plane is damaged and severe when 3/12 or more of the sphincter in the transversal plane is damaged [14]. The women were counselled for vaginal delivery or a primary caesarean section based on their symptoms and the sphincter defect classification of the EAUS [14], [15]. During this counselling, the women were informed about the risk of FI in the future and the disadvantages and risks of a primary caesarean section. The disadvantages of the EAUS are that the probe must be inserted into the anal canal and shows a transversal 2D image. For a correct sphincter analysis, it is necessary to move the probe and estimate which part of the length of the sphincter is damaged. Additionally, the analysis is only done on the anatomy of the sphincter and not based on the sphincter's function, which is essential information.

The function of the external anal sphincter can be measured using anorectal manometry, EMG assessment (e.g. MAPLE) or manually. A balloon, probe or finger must be inserted into the anal canal to measure the pressure or signal during contraction for all these methods. However, these methods give less or no information about the anatomy of the sphincter. A study by Jordan et al. [15] has shown that manometry in combination with EAUS can help by counselling for the delivery mode. However, this means an additional diagnostic device must be inserted into the anal canal. Additionally, the manometry takes 30 to 45 minutes, which is relatively long.

To be able to assess the EAS anatomy and function, a new promising technique is considered, namely 3D transperineal ultrasound (TPUS). This technique is a less invasive method due to positioning the probe on the perineum instead of inside the anal canal. It gives comparable anatomical results of the EAS with 2D EAUS [16], [17]. Additionally, it can quantitatively assess the pelvic floor's motion in 3D during contraction or Valsalva. To our knowledge, Das et al. [18] was the first study that quantitatively determined the function of the PRM based on strain measurements. Strain is the deformation of the muscle's volume over time. They assessed the 3D displacement and strain in the PRM during contraction and Valsalva measured with 3D TPUS [18]. This method is also called 4D TPUS due to the analyses of the 3D volume over time, so time is the fourth dimension. A study by Hölscher et al. [19] measures the EAS thickness at 6 and 12 o'clock and the change in the diameter of the anal canal between rest and contraction with perianal tomographic ultrasound images. However, this was not a quantitative measurement of the whole EAS, and there were no measurements on the left and right EAS parts. It would be interesting to know if 3D displacement calculations between rest and contraction can also assess the EAS function. Healthy nulliparous women are chosen to understand what happens with the EAS between rest and contraction in healthy EAS. That are women who have not yet given birth, so these EAS are considered intact and healthy. Therefore, this pilot study gives insight into a normal EAS function determined with 3D displacement calculations. Additionally, it is interesting to investigate if there are differences between EAS function measured with 4D TPUS between healthy women and women with previous OASI. Therefore, women with previous OASI are also used in this study. We hypothesized that differences in EAS function would be assessed with 4D TPUS with 3D displacement calculations.

Summarized, the first aim of this pilot study is to assess the technical feasibility of EAS segmentation and 3D displacement assessment. The second aim is to get insights into the displacement outcomes of EAS during contraction in healthy nulliparous and in women with previous OASI and compare both results if there are differences.

2. Materials and methods

2.1. Study population

This prospective pilot study was conducted with patients and controls. All women had a good knowledge of the Dutch language and were 18 years or older. The patients consisted of women with previous OASI from the gynecology department of ZGT hospital in Hengelo and Almelo, who were planned for 2D EAUS. The exclusion criterium of the patient group is a previous sphincter surgery. The controls consisted of women who had never given birth (nulliparous), had never been pregnant, and were enrolled via flyers. The exclusion criteria of the control group are a gestation > 14 weeks, symptoms of pelvic floor dysfunction (e.g. urinary or fecal incontinence) or known sphincter injury.

2.2. Data acquisition/collection

The 4D TPUS volumes were acquired with the EPIQ 7G US machine using the Philips X6-1 matrix transducer at the ZGT. All the patients and controls were scanned in a supine position, and a gel pad with a thickness of 2 cm was added between the probe and the patient. The final gel pad construction is shown in Figure 2. The gel pad ensures the whole sphincter complex is in the field of view during contraction. The probe consisted of 9212 elements, the volume angle was 90 degrees in both orthogonal directions, the scan depth was 9 cm, the framerate was 3Hz, and the post-processing filters were set off.

The ultrasound protocol was optimized during the data collection resulting in variations in the data of the patient group. The resolution varied in the patient group between 0.75-0.83 mm between the 256 X-slices, 0.48-0.53 mm between the 185 to 187 Y-slices and 0.43-0.44 mm between the 222 to 234 Z-slices. The last 41-47 frames of the 4D measurement were saved. All the nulliparous data were collected with the final ultrasound protocol. The resolution of the frames collected with the final protocol was 0.75 mm between the 288 X-slices, 0.50 mm between the 186 Y-slices, and 0.43 mm between the 226 Z-slices. The last 41 frames of the 4D measurement were saved.

During the TPUS assessment, two 4D measurements were made of the anal sphincter complex. Figure 2 visualises the probe's position on the perineum during the TPUS assessment. During the measurements, they were asked to contract the pelvic floor how they would hold their defecation, hold this for 2 seconds, and relax again. The measurement was stopped 2 seconds after the relax instruction, and the 4D measurement was saved consisting of rest to contraction and back to rest. Figure 3 shows the TPUS images of the anal sphincter complex during rest in sagittal and transversal view. The EAS is a hyperechogenic (white) structure, while the IAS is a hypoechogenic (black) structure.

Figure 2. Probe position on the perineum for the measurement of the anal sphincter complex (A)[24] *and the gel pad added on the probe with a glove around it and fixed with tape(B).*

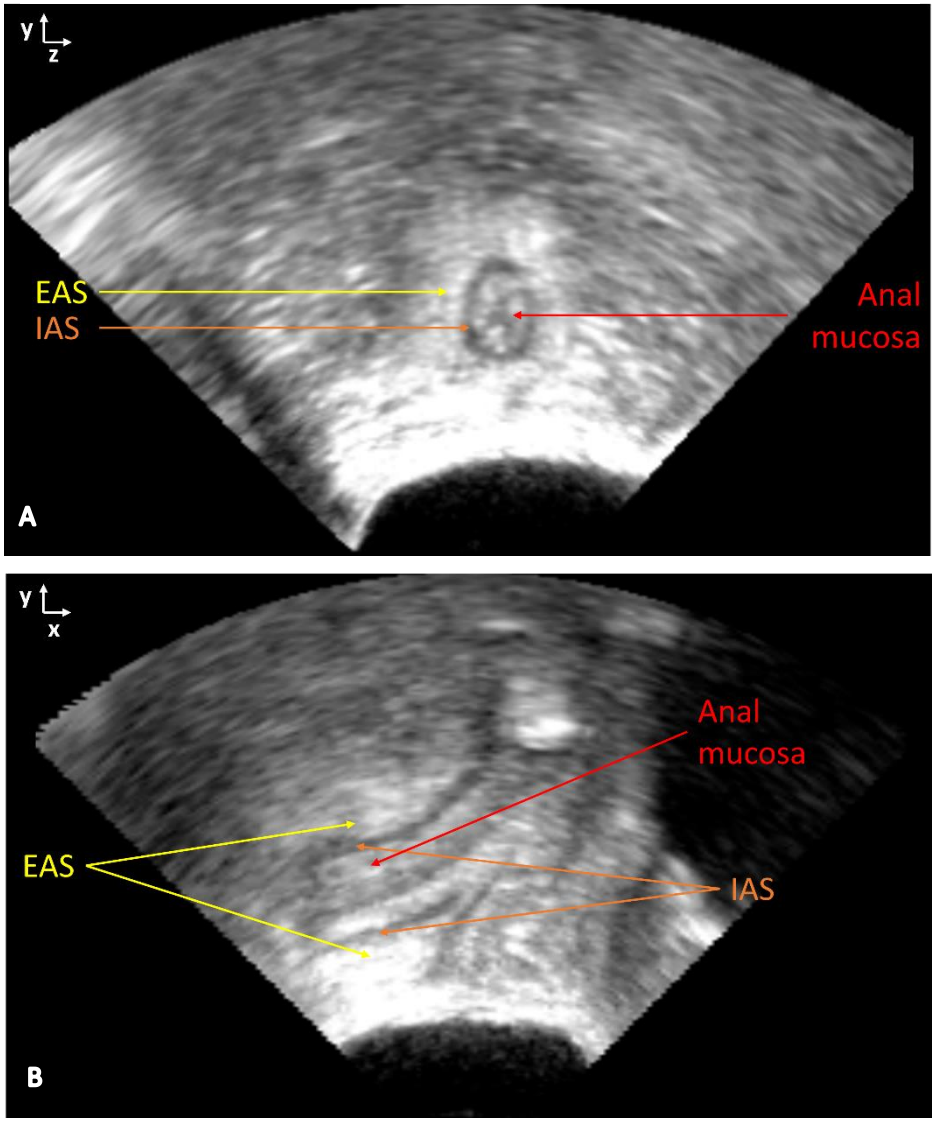

Figure 3. TPUS images of anal sphincter complex in transversal (A) and sagittal view (B). The hyperechogenic structure is the EAS (yellow arrow), and the hypoechogenic structure is the IAS (orange arrow). Inside the IAS is the anal mucosa visible (red arrow).

2.3. Data processing

Data preparation

Input data for the displacement calculations are original data of the US machine, a conventional DICOM format and the manually segmented region of interest (ROI) of the EAS in the restframe before contraction.

The original US machine data of the 4D measurements were in DICOM format. However, these data must first be converted to a file with the '.fld' extension before it can be used in MATLAB. This conversion was done with QLAB, version 15.5 (Philips Healthcare, Andover, MA,USA). The conversion to a conventional DICOM file was done in MATLAB. QLAB was used to determine the rest frame before the contraction and the frame with maximum contraction. The DICOM file of the rest frame is extracted from all the frames to use for segmentation of the EAS with MATLAB.

3D EAS segmentation

The EAS sphincter is manually segmented in the restframe before the start of contraction in 3D Slicer version 5.2.1.. Proper guidelines on 3D segmentation of the EAS are lacking. An in-house 3D segmentation protocol is developed to ensure adequate and reproducible results. This protocol is based on published 2D segmentations in previous papers [20], [21], anatomical information of the EAS in previous papers [22] (Appendix A), a TPUS expert meeting, and our own clinical experience with assessing EAUS anatomy. The protocol is stated as follows:

Step 1: Rotate the slice toward the anal canal in the sagittal and coronal views (Figure 4). This rotation ensures that the EAS can be determined over these axes in the transversal view, making it most comparable with the EAUS (the golden standard).

Step 2: Set the upper boundary of the EAS in the transversal view. The upper boundary is determined at the slice of opening the EAS and merges into the PRM in the transversal view (Figure 5).

Step 3: Set the lower boundary of the EAS in the transversal view. The lower boundary is determined at the last slice, where the internal anal sphincter is visible in the transversal view in combination with the sagittal and coronal view (Figure 6).

Step 4: Set the thickness of the EAS in different views by setting the inner (step 4a) and outer boundary of the EAS (step 4b). Figure 7 shows the segmentation of the thickness of the EAS. The thickness is first determined in the transversal view and checked in the sagittal and coronal view. **Step 4a:** Set the inner boundary of the EAS. The inner boundary is the edge of the IAS. The IAS has a hypoechogenic structure, and the EAS is a hyperechogenic structure. This difference ensures a good distinction between both structures. **Step 4b:** Set the outer boundary of the EAS. The outer boundary can be determined due to following the white colour on the left and right sides of the EAS to the anterior and posterior parts. The distinction between the EAS and other muscles is more difficult in the anterior and posterior parts of the EAS than in the left and right. Especially for the outer boundary, it is essential to check the muscle in the other directions to see if another muscle or structure is segmented instead of the EAS.

Step 5: Smooth the segmentation boundaries using the Gaussian smoothing method with a standard deviation of 1 mm.

The segmentation of a patient with a previous OASI consists of the same steps of the healthy segmentation protocol. However, the segmentation is more difficult in these data due to the OASI part. The OASI part is defined by an interruption of the hyperechogenic EAS, which is visible as a hypoechogenic structure. The OASI part will also be segmented in the whole EAS segmentation.

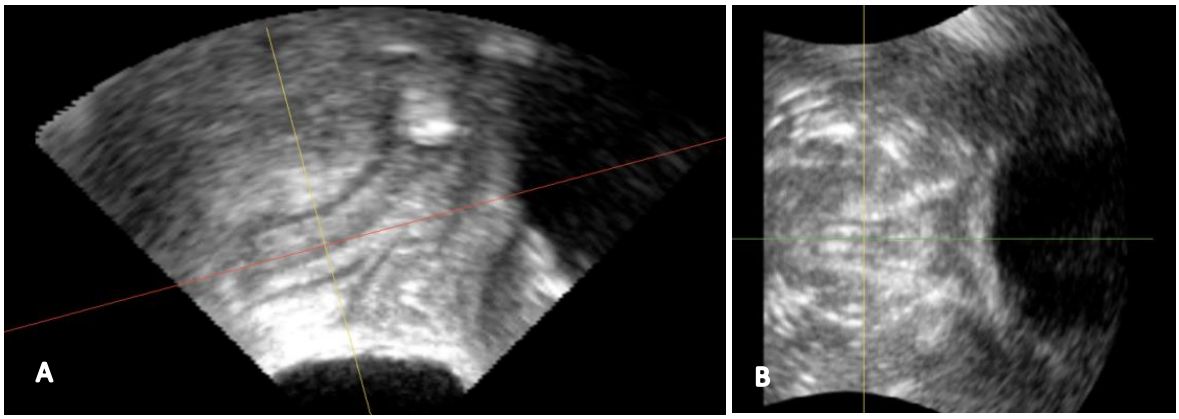

Figure 4. The rotation into the anal canal. The red line is the rotation in the sagittal view (A), and the green line is the rotation in the coronal view (B).

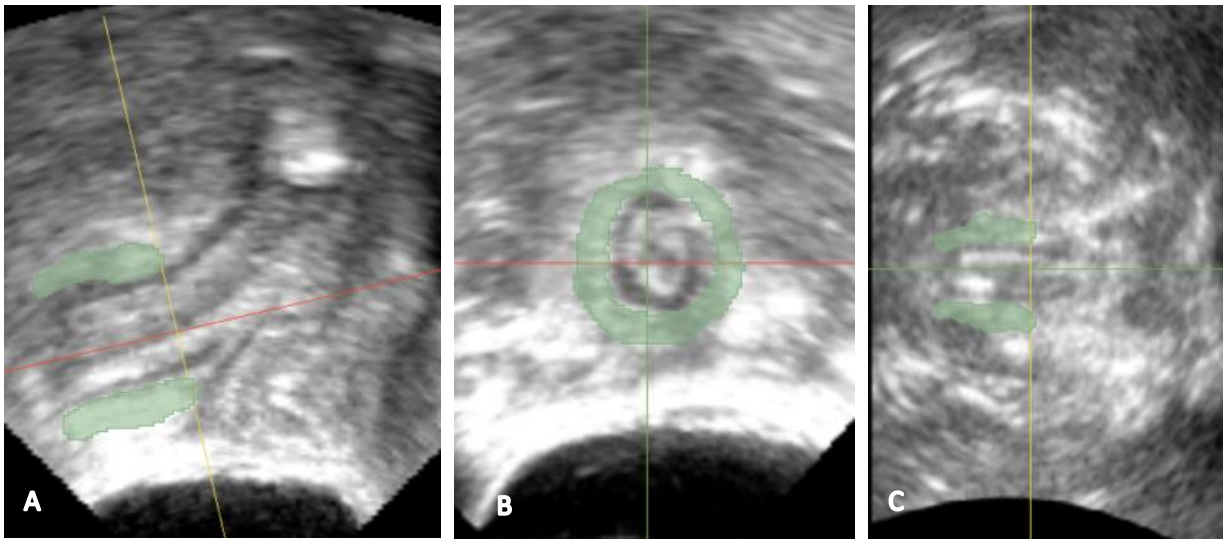

Figure 5. Upper boundary segmentation in sagittal (A), transversal (B) and coronal (C) views of the EAS in green. The yellow line in the sagittal and coronal view corresponds with the plane in the transversal direction.

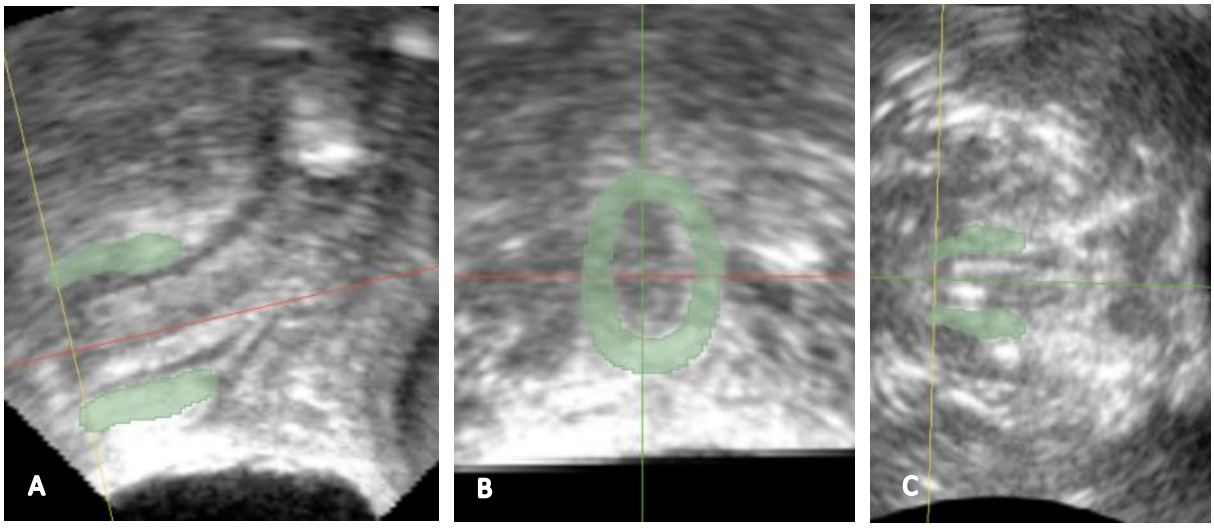

Figure 6. Lower boundary segmentation in sagittal (A), transversal (B) and coronal (C) views of the EAS in green. The IAS is still minimally visible in the transversal slice, and it is still visible in the coronal slice.

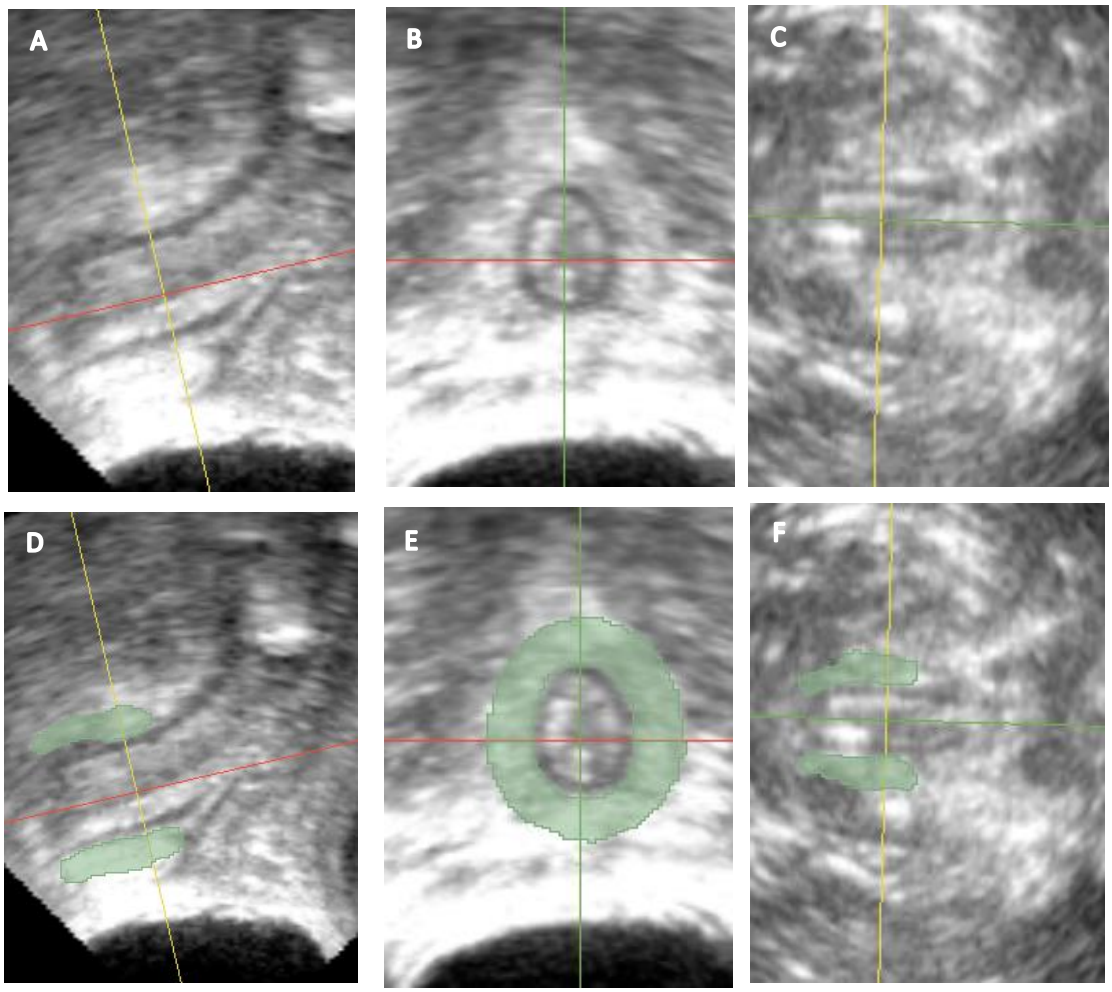

Figure 7. TPUS images without (A, B, C) and with the segmentation (green volume in D, E, F) to illustrate the thickness of the EAS in sagittal (A, D), transversal (B, E) and coronal (C, F) views.

Displacement software

A part of the strain software of Das et al. [18] is used to calculate accumulated displacement estimates in the EAS. The input of this software is the original US machine data, the conventional DICOM data and the manually segmented EAS ROI. Figure 8 shows the most important steps of this software.

The first step of the software was to calculate inter-volumetric displacements. In this step, the displacement of the ROI between the selected rest frame and the subsequent frame is estimated with a 3D normalized cross-correlation algorithm optimized for PF muscles and the US system by Das et al. [18]. The only change in the software for the EAS was modifying the kernel size and template size to 61x61x61 and 41x41x41, respectively, because of the other shape of the EAS than the PRM. This algorithm calculates the displacement for each two subsequently recorded frames.

The EAS changes in position during contraction so between the different frames. Therefore, it is important to change the initial ROI position over the following frames. Because if the initial ROI position of the first frame is used in calculating the displacement between frames 4 and 5, the EAS not located at the initial ROI position due to the movement during contraction. So then another structure than the EAS is tracked. For that reason, the second step is tracking the muscle. Tracking means that the initial ROI will be updated using the estimated displacement of step 1. These steps are repeated till the last frame and are also in the software of Das et al. [18].

The estimated displacements were calculated in each direction. These values between the different frames can be used to calculate the accumulated displacement estimates in the x-, y- or z-direction to take the sum of the estimated displacement of the rest frame until the contraction frame. More details about the software can be found in the article of Das et al. [18].

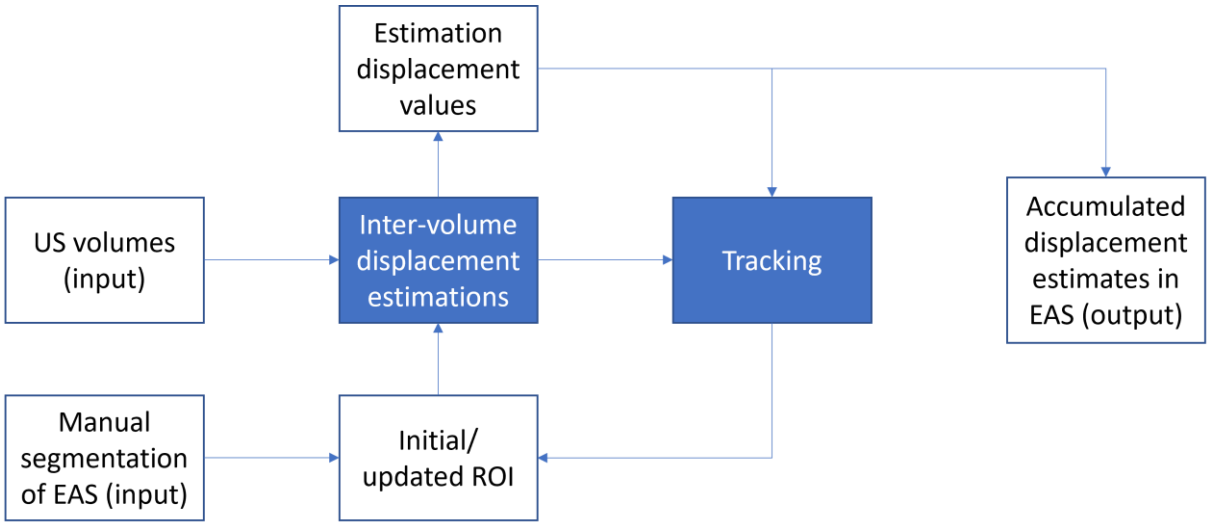

Figure 8. Visualisation of the most important steps to calculate the accumulated displacement estimates.

2.4. Data analysis displacements

The accumulated displacements values are visualised in a scatterplot. A scatterplot consists of the accumulated displacement between rest and maximum contraction in the x-, y-, or z-direction. The displacement will be visually analysed individually in three directions in the control group, in the patient group and between both groups to compare the most representative control and patient.

6D data (a 3D structure with three displacement directions) is challenging to analyse and compare, so it is chosen first to analyse all displacement directions in the middle transversal frame of the length of the EAS. The last updated ROI is used to determine this middle frame to determine the lowest and maximum x-coordinate value of the ROI, and then it is known at which x-value is the middle frame. Figure 9 shows a visualisation of the middle frame of the EAS length.

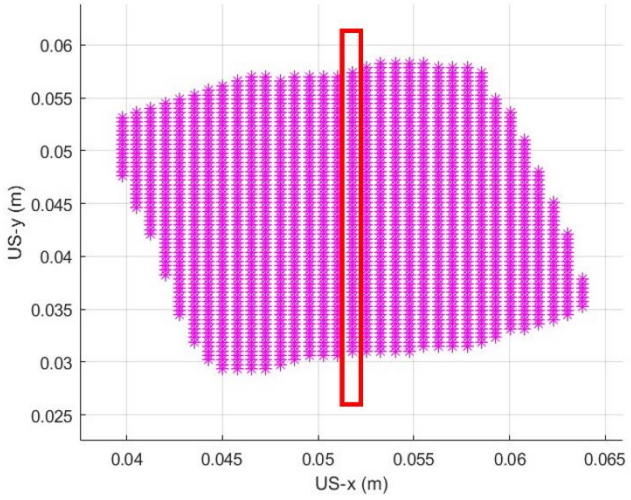

Figure 9. Visualisation of the middle frame of the length of the EAS. The US-x axis is the direction of the EAS length. The red box is the selected middle frame.

3. Results

Figure 10 shows the flowchart of the included patients with previous OASI. The TPUS was conducted on 13 patients. 8 patients were excluded from the study based on poor image quality (n = 6), too much damage in IAS and EAS to distinguish EAS to make the segmentation (n = 1) and an error during voxel tracking due to EAS position and the used kernel- and template size (n = 1). The displacements are calculated for 5 patients with previous OASI. 5 nulliparous controls were included and the displacements are calculated in all of these controls. Table 1 summarizes the demographic characteristics of the patients and controls.

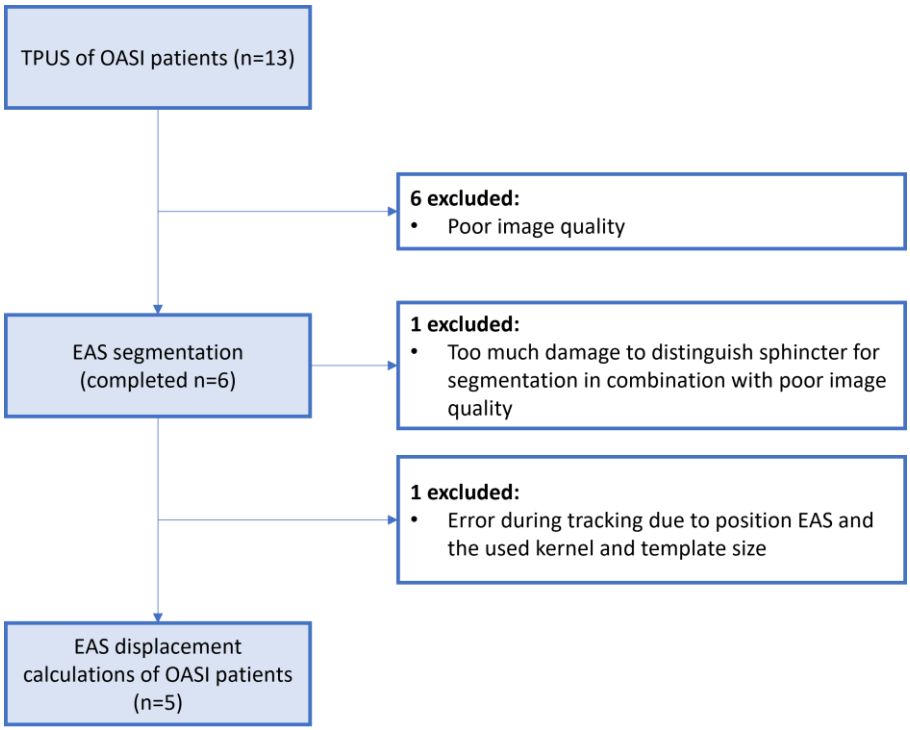

Figure 10 . Flowchart of the included OASI patients.

*Table 1. Overview of the demographic characteristics of the patient and control group. * wrong grade 2 grading after vaginal delivery, EAS damage on EAUS.*

	Age (yr)	Gravida	Para	Grade OASI	Complaints of FI	Postmenopausal
Patient 1	38	3	2	3A	Yes, FI for fluid	No
Patient 2	28	2	1	3B	No	No
Patient 3	31	6	2	3A	Yes, FI for gasses	No
Patient 4	29	2	2	2*	Yes, FI for fluid and gasses	No
Patient 5	31	2	1	3A	No	No
Control 1	24	0	0	-	No	No
Control 2	55	0	0	-	No	Yes
Control 3	22	0	0	-	No	No
Control 4	60	0	0	-	No	Yes
Control 5	20	0	0	-	No	No

3.1. Segmentation

The 3D segmentation and corresponding transversal view of 1 control are illustrated in Figure 11. A complete overview of all controls, including sagittal and coronal views, can be found in Appendix B.

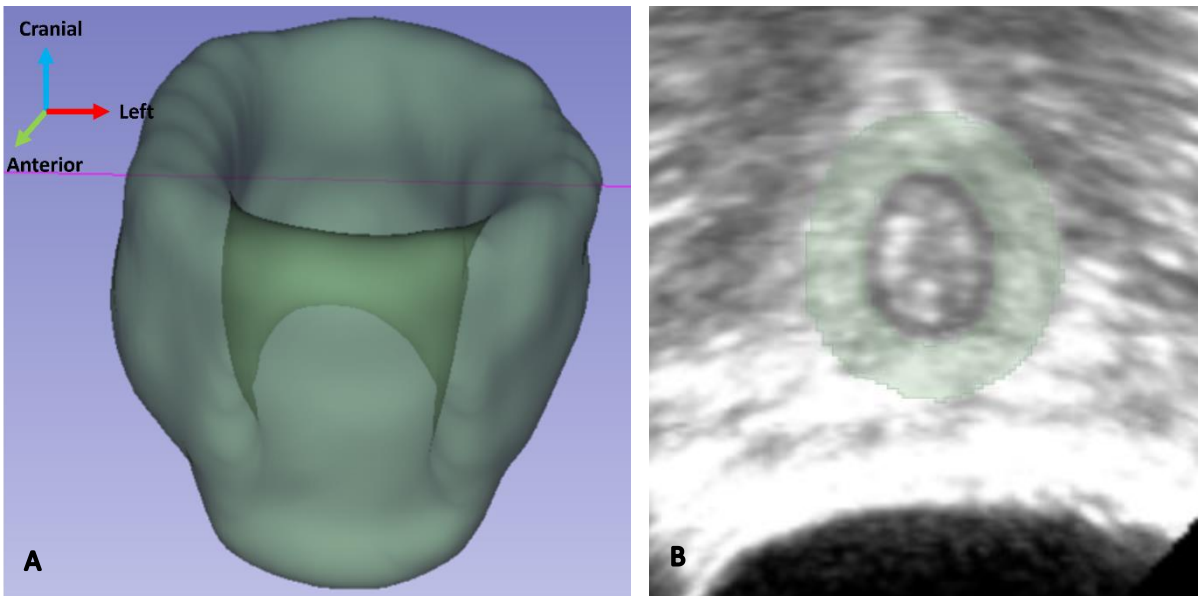

Figure 11. The 3D view of the segmentation of a control (A), and a transversal slice of the segmentation in the ultrasound image (B). The segmentation of the EAS in green.

The 3D EAS and OASI segmentation and corresponding transversal view of 1 patient are illustrated in Figure 12. A full overview of all patients, including sagittal and coronal views, can be found in Appendix C.

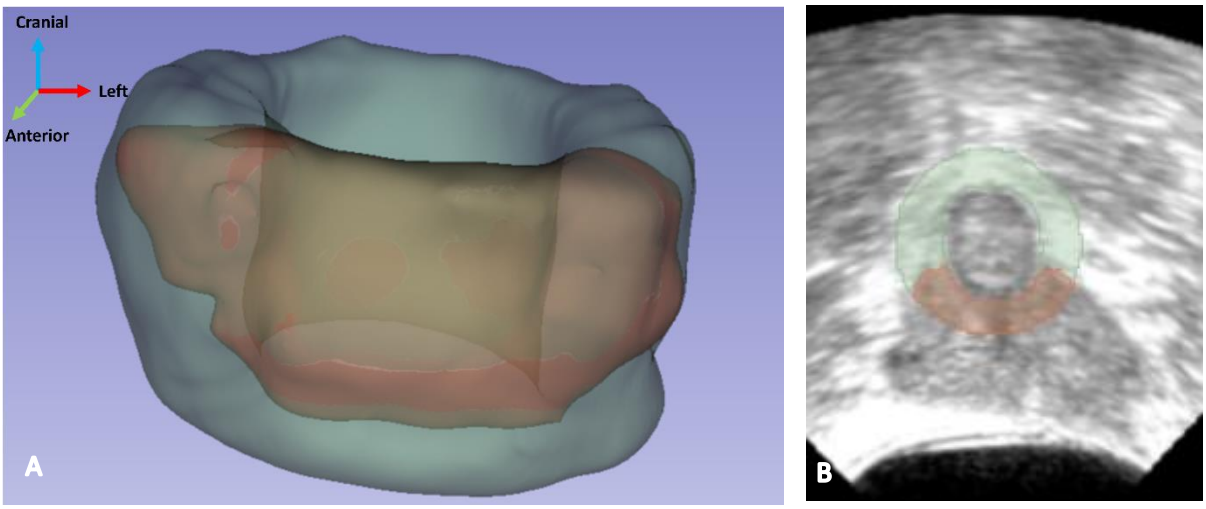

Figure 12. The 3D view of the segmentation of a patient (A), and a transversal slice of the segmentation in the ultrasound image (B). The segmentation of the EAS, including OASI, is in green, and the sub-segmentation of the OASI part is in red.

3.2. Orientation sphincter

Figure 13 shows the defined orientation in the TPUS images and the US coordinate system. The x-axis is defined as the caudal-cranial direction, and a lower x-coordinate is the caudal part of the EAS. The y-axis is defined as the anterior-posterior direction, and a lower y-coordinate is the anterior part of the EAS. The z-axis is defined as the right-left direction, and a lower z-coordinate is the left part of the EAS. The axis in the transversal view between the TPUS images and the US coordinate system is rotated.

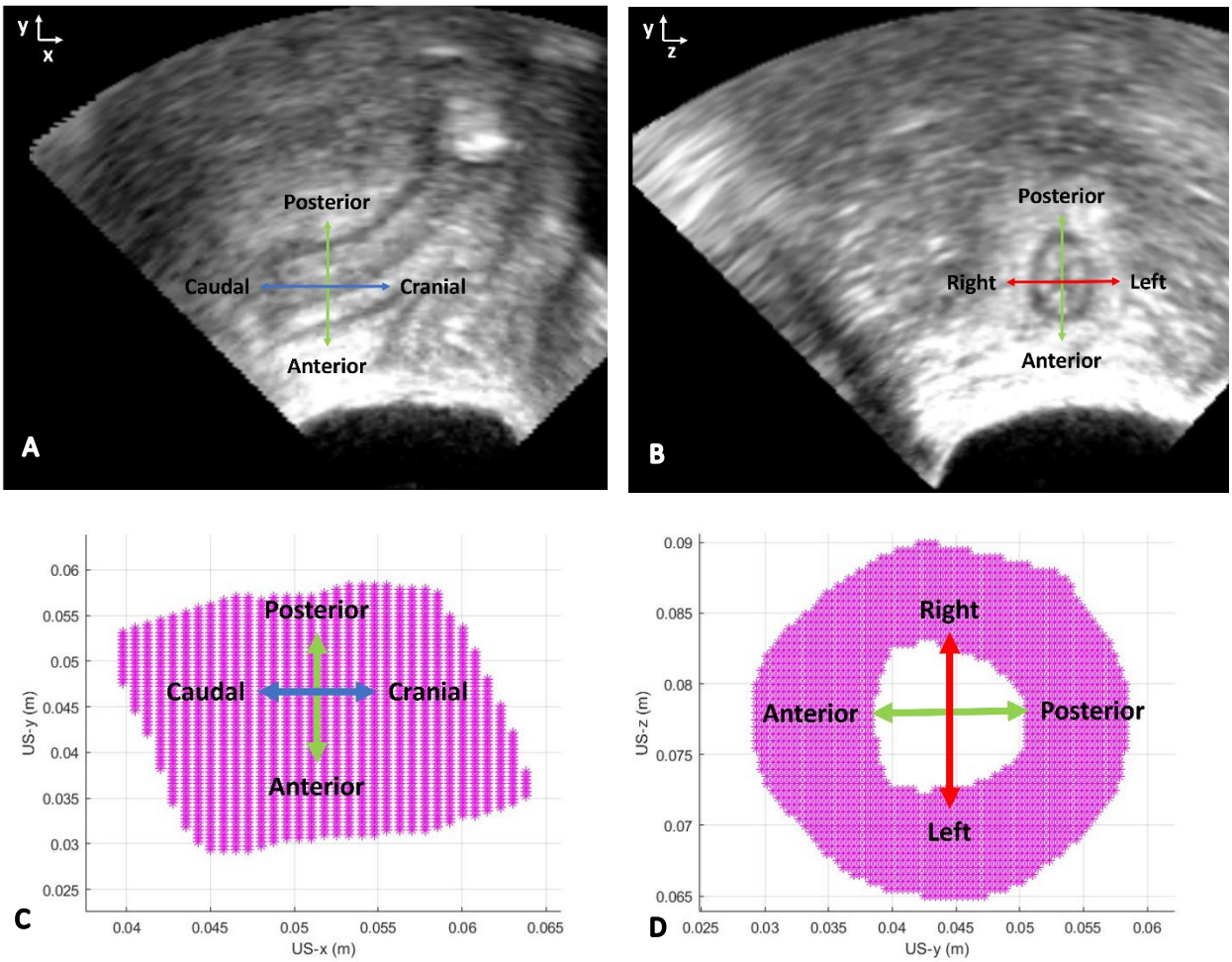

Figure 13. TPUS images of the anal sphincter complex in sagittal (A) and transversal view (B) and the orientation of the EAS segmentation in the US coordinate system (C,D). The blue double-headed arrow in the sagittal view represents the caudal-cranial direction. The green double-headed arrow represents the anterior-posterior direction. The red double-headed arrow in the transversal view represents the right-left direction.

3.3. Displacement controls

The displacement in the x-, y-, and z-direction of each voxel of the segmented EAS in a 3D view of one control are visualised in Figure 14. It shows that the estimated displacements are the highest in the direction of the x-axis. These displacements are positive values representing the movement to the cranial direction. The estimated displacements of the y-axis are also all positive values, representing a movement to the posterior direction. The displacements of the z-axis consist of positive and negative values. The positive voxels move to the right part of the sphincter, and the negative voxels move to the left part. Additionally, the different colours of the displacements differ slightly in the EAS length (x-axis).

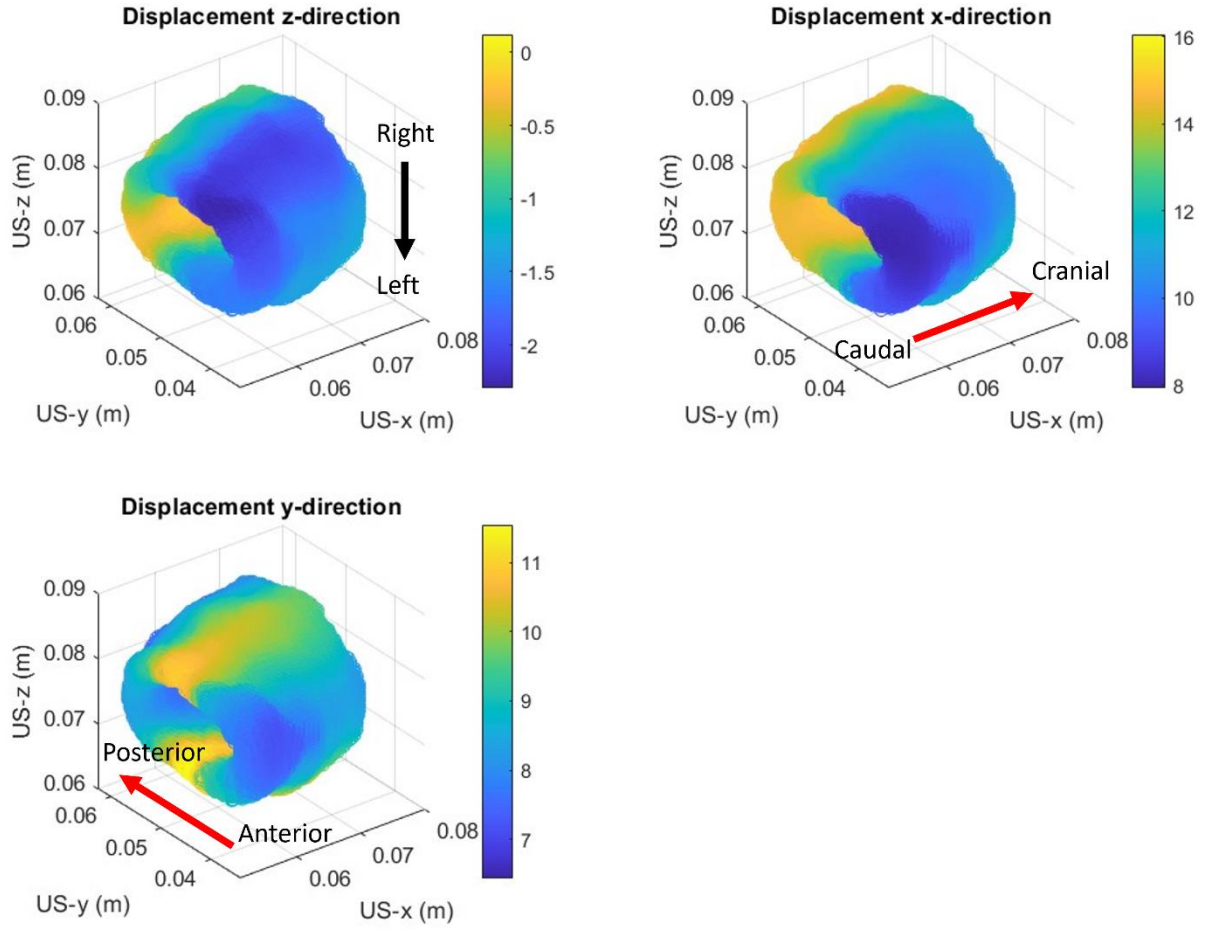

Figure 14. A visualisation of the displacement estimates in the x-, y-, and z-axis of the 3D EAS from rest to maximum contraction in one control. The colours of the image display the displacement of that specific direction in mm. A positive displacement value is a movement of that specific voxel to a higher value in that axis (red arrow). The black arrow shows the direction of a negative displacement.

Figure 15 shows the displacement of the voxels between rest and the maximum contraction of one transversal slice in the middle of the EAS length of all controls (Appendix D). The scale of the colour bar differs between the different controls due to different maximum and minimum displacement values in the specific direction. The displacements in control 2 are in all directions less than in the other four controls. However, the maximum displacement value in all control is the highest in the x-direction and all positive, so the EAS moves the most in the cranial direction. It also shows that **the displacement in the x-direction** is the largest in the posterior part of the EAS, so the posterior part moves more in the cranial direction than the anterior part of the EAS.

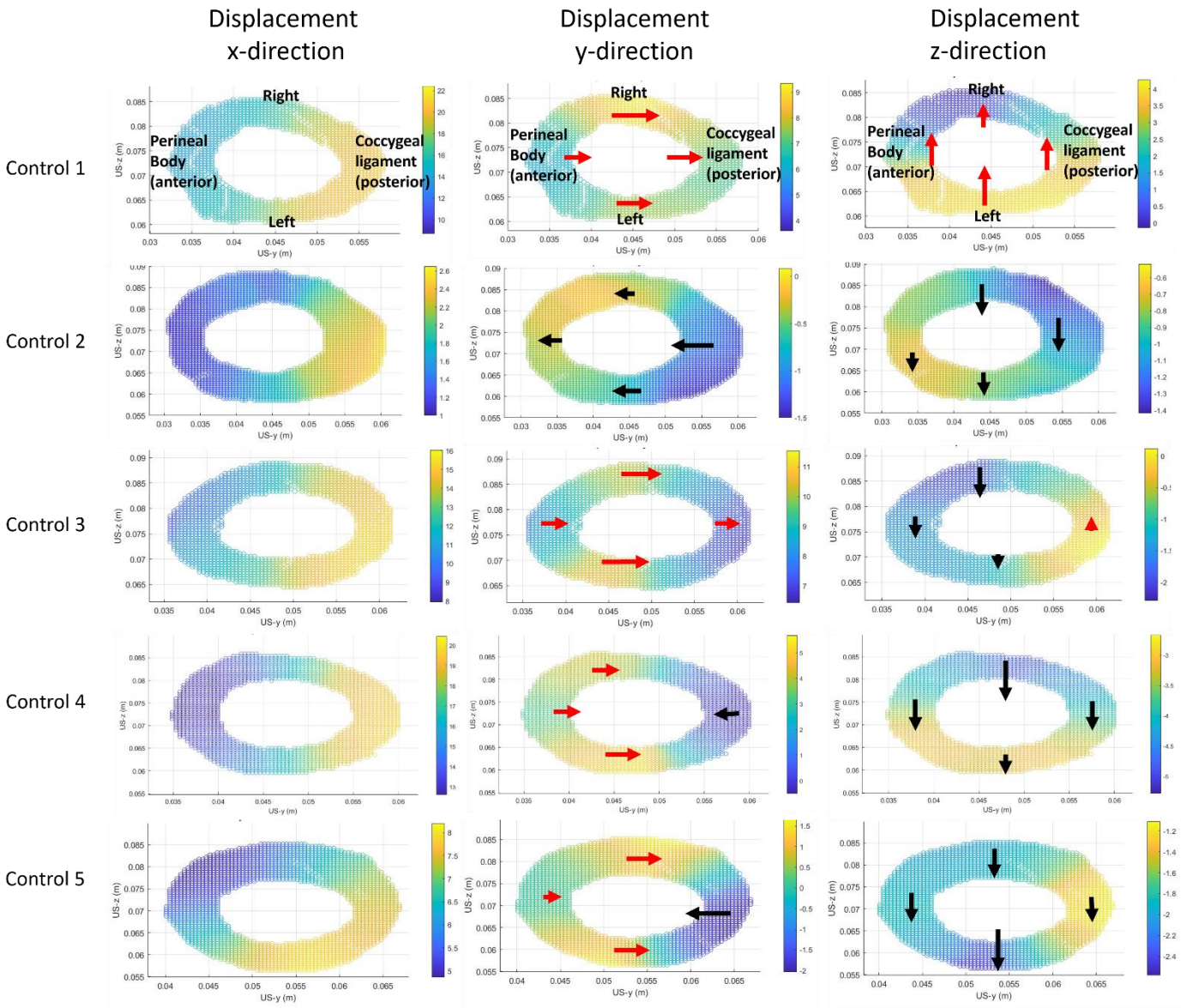

Figure 15. The x-, y-, and z-displacement of the voxel in the middle slice of the sphincter in the transversal view of all the controls. The colours of the image display the displacement of that voxel in the specific direction in mm. The highest displacement value of a control in the specific direction is visualised in yellow, and the lowest value is in blue. The red arrows represent a positive displacement in that axis, and the black arrows represent a negative displacement. The length of the arrow is based on the extent of displacement of that control.

The displacement in the y-direction shows that this is only positive in control 1 and 2, positive and around zero in control 4, negative and around zero in control 3, and positive and negative in control 5. Additionally, the anterior and posterior side of the EAS moves to each other in control 2, 3, 4 and 5. While the posterior part moves more to the posterior side than the anterior part of the EAS in control 1, so both parts move away from each other during contraction. Most displacement during contraction in the y-direction is in all controls' the left or right EAS part.

The displacement in the z-direction shows that this is only positive in control 1, only negative in controls 2, 4 and 5, and negative and around zero in control 3. Additionally, it shows that the right part moves more to the left than the left part in controls 2, 3, and 4. While in control 1, the left part moves more to the right than the right part of the EAS. Further, in control 5, the right part moves less to the left than the left part of the EAS. So in 4 out of 5 controls, the right and left parts move to each other during contraction.

3.4. Displacement OASI

Figure 16 shows the displacement of the voxels between rest and the maximum contraction of one transversal slice in the middle of the EAS length of all patients (Appendix E). The scale of the colour bar differs between the patients due to different maximum and minimum displacement values in the specific direction. In patients 3 and 4, the maximum displacement is the highest in the x-direction, so the EAS moves the most to the cranial direction in these patients. In the other three patients, the maximum displacement is the highest in the y-direction, so the EAS moves the most to the right in these patients.

The displacement in the x-direction is in all patients higher in the posterior part than in the anterior part of the EAS, so the posterior part moves more in the cranial direction than the anterior part of the EAS. Additionally, this displacement is the same in the right and left part of the EAS as the posterior part in patient 1, and the left part of the EAS moves more to the cranial than the right part in patients 3, 4, and 5.

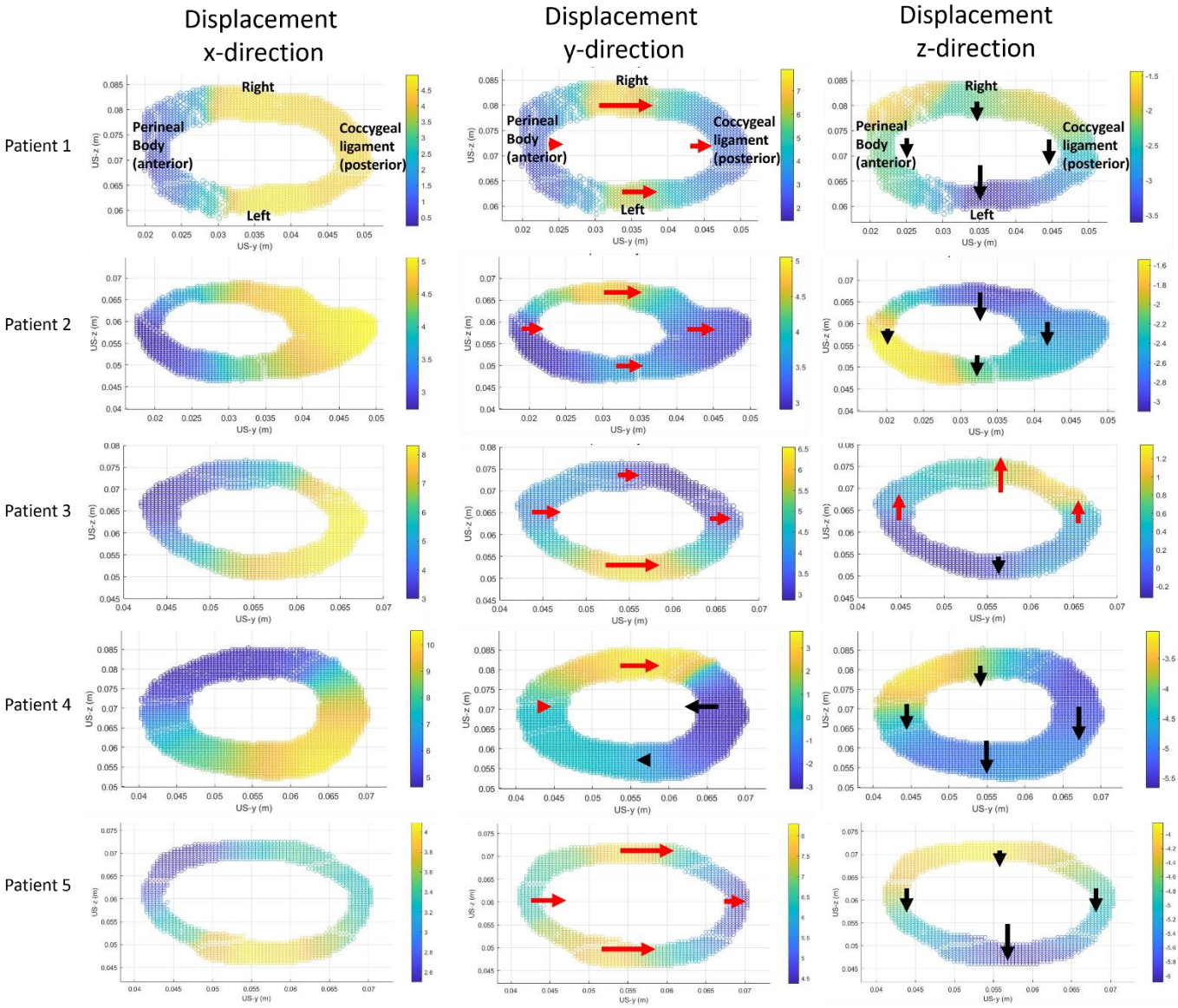

Figure 16. The x-, y-, and z-displacement of the voxel in the middle slice of the sphincter in transversal view of all the patients. The colours of the image display the displacement of that voxel in the specific direction in mm. The highest displacement value of a patient in the specific direction is visualised in yellow, and the lowest value is in blue. The red arrows represent a positive displacement in that axis, and the black arrows represent a negative displacement. The length of the arrow is based on the extent of displacement of that patient.

The displacement in the y-direction is in all voxels positive in patient 1,2,3 and 5, and positive as well negative in patient 4. Additionally, it shows that in patient 1, 2, and 3 the displacement values in y-direction are approximately equally positive in the anterior part as the posterior part. While in patient 4, the displacement value in the anterior part is around zero and the posterior side has a negative displacement, so moves to the anterior side. And in patient 5, the displacement in the anterior part has a higher positive value than in the posterior part. So in three patients the y-displacement in anterior and posterior side are comparable and in two patients the anterior and posterior side are closer together at maximum contraction compared to rest.

The displacement in the z-direction is positive and negative in patient 3 and negative in the other patients. Additionally, the displacement in the z-direction has a less negative value in the right part of the EAS compared with the left side in patients 1, 4, and 5. In patient 2, the right part has a more negative displacement than the left part of the EAS. Moreover, in patient 3, the right part has a positive displacement while the left part has a negative displacement. So the left and right parts are more apart at maximum contraction than in rest in 4 out of 5 patients, only not in patient 2.

3.5. Comparison control and patient

Figure 17 shows the displacement of the voxels between rest and the maximum contraction of one transversal slice in the middle of the EAS length of control 3 and patient 3. The maximum displacement in the x- and y-direction are higher in control 3 than in patient 3. **The displacement in the x-direction** is higher in the posterior part than in the anterior part in the control and in the patient. In control, the displacement in the x-direction is more symmetrical in the left and right parts than in the patient.

The displacement in the y-direction is in control 3 higher in the anterior part of the EAS than in the posterior part, while these displacements are more comparable in both parts in patient 3. Additionally, the displacement in the y-direction is in the control reasonably comparable in the left and right parts. In contrast, in the patient, this displacement is higher in the left part than in the right part of the EAS.

The displacement in the z-direction is mostly negative or around zero in control 3 and mostly positive and minimally negative in patient 3. The right part of the EAS moves to the left in control 3, while in patient 3 this part moves to the right. Additionally, the anterior part moves to the left in control 3, while it moves minimally to the right in patient 3. The left and posterior part moves fairly similarly in control 3 and patient 3. Due to a movement in another direction in the right part of the EAS, the left and right parts are closer together during maximum contraction compared to rest in control 3, while in patient 3 the left and right parts are further apart during maximum contraction than in rest.

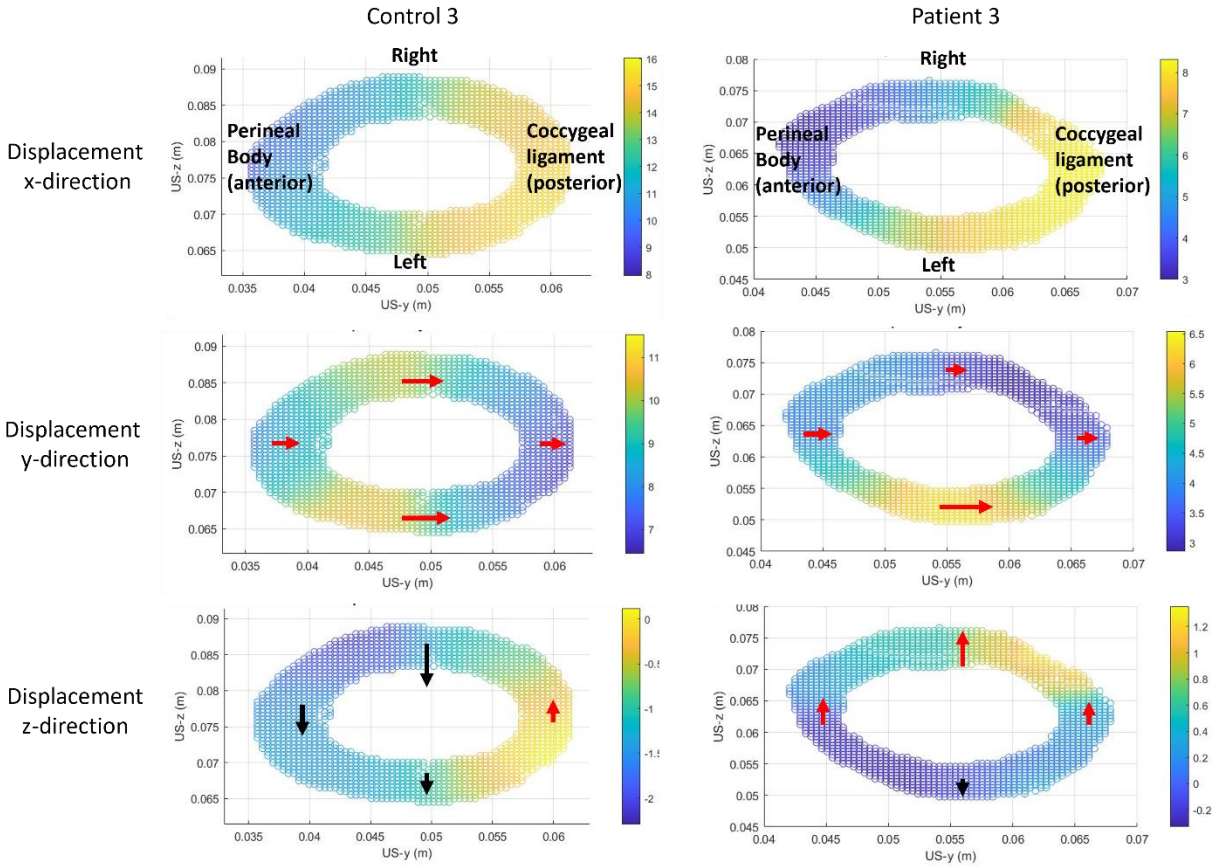

Figure 17. The x-, y-, and z-displacement of the voxel in the middle slice of the sphincter in transversal view of control 3 and patient 3. The colours of the image display the displacement of that voxel in the specific direction in mm. The highest displacement value of a patient in the specific direction is visualised in yellow, and the lowest value is in blue. The red arrows represent a positive displacement in that axis, and the black arrows represent a negative displacement. The length of the arrow is based on the extent of displacement of that patient.

4. Discussion

This pilot study shows that it is technically feasible to segment the EAS and determine 3D displacements. In most controls, during contraction, a cranial movement of the whole sphincter, closing of the left and right parts, and closing of the anterior and posterior parts are found. In most patients, during contraction, an asymmetrical movement of the left and right parts in the cranial and posterior direction and openings of the left and right parts are found. There were differences in comparing the control and patient, which is very promising for the future.

4.1. EAS segmentation

The EAS consists of different parts; ideally, the full EAS is assessed during the displacement calculations. Due to technical limitations (e.g. difficult to distinguish the subcutaneous part of the EAS due to less space between the EAS and no IAS), only the superficial and deep parts of the EAS were included in the segmentation. Additionally, the deep part of the EAS merges into the PRM. In the current segmentation protocol, the segmentation ended cranial where the EAS opened on the anterior side, while it is known that the posterior part of the EAS is longer than the anterior side in women [22]. It is anticipated that the lack of these segmentations will not have influenced these results since adding these parts will give additional information of these parts and not give other displacement values of the currently used segmentations.

The EASs of patients are more difficult to segment due to the damage to the sphincter. Ideally, the correct EAS parts were segmented and assessed during the displacement calculations. However, it is sometimes difficult to distinguish the EAS from the surrounding tissues. There could be scar tissue between the EAS parts that attached the parts, but another option could be that a part of the EAS is not attached to the other EAS part. The segmentation protocol could be adjusted to stop the segmentation when there is a sign of a retracted muscle with a higher density, resulting in a non-circular EAS segmentation. Additionally, the OASI is always located on the anterior side of the EAS. This location provides a more difficult segmentation on the deep EAS part because the EAS will also open in that part. So, it is sometimes difficult to distinguish between scar tissue and opening the EAS. Further, one patient was excluded due to too much damage on the EAS and IAS to segment the EAS because it cannot be distinguished properly. This patient shows that, in some cases, the TPUS is more difficult to interpret than the EAUS. However, the image quality was also poor due to insufficient ultrasound gel, causing signal loss and artefacts. This quality could also be a reason why it was difficult to distinguish the EAS for segmentation. Lastly, the segmentations are not checked by another expert, but doubts about the segmentation of the patients are discussed with another expert. So, there were still some doubts or improvement points in the EAS segmentations. However, most parts of the sphincters were segmented well, which are reliable for displacement calculations.

4.2. Displacements

To our knowledge, this study was the first study to assess a quantitative 3D displacement of the EAS. The results show a variation in displacement value in the different controls. The women who indicated difficulty with contracting her sphincter also had low displacement values. This supports the conclusion that quantitative 3D displacement of the EAS is feasible.

The results show a large displacement of the EAS in the cranial direction of the controls. This displacement cannot be due to the EAS itself because this is the movement in the EAS length, and the EAS is a more circular muscle. It could be the effect of the PRM contraction because the PRM will also be contracting when contracting the pelvic floor to hold the defection. The PRM lies with a sling around the posterior part of the anal canal and is attached to the pubic bone. When contracting the PRM, the anorectal angle will be sharpening, resulting in the anus and thus, the EAS will be moved in the cranial

direction defined in the US images. This can also clarify why the posterior part moves more in this direction than the anterior part of the EAS. Therefore, the displacement in the z-direction (cranial-caudal direction) is unimportant for the EAS function. However, also the PRM function is important to maintain fecal continence.

The displacement in the y-direction, in the anterior-posterior axis defined in the US image, was higher in the left and/or right part of the EAS than in the anterior and posterior parts. This could be because the anterior and posterior are attached to the perineal body and coccygeal ligament, respectively. There may be less movement due to these attachments and more movement in the left and right parts. Further, in control 1, the anterior and posterior parts are more apart during contraction than in the other controls. It was seen that the tracking of the anterior part of the EAS was the worst when analysing the certainty of the tracking. Control 1 made a good and fast contraction of the pelvic floor. This fast contraction can make it more difficult to track the muscle.

In the displacement in the z-direction, left-right axis, the results show in the control group that the left and right parts are closer together during contraction. However, the amount that both parts come closer together is minimal between the 1 and 4 mm in the control group. On the other hand, this already gives new insights into the movement of the EAS during contraction. Further, the movement in the z-direction in most patients is that the left and right are opening, so the opposite happens. In patient 2, this displacement was not different from the controls. However, the EAS was very skewed in the 4D TPUS images, which can give other results since the displacements were calculated in the US coordinate system.

In the comparison of control 3 and patient 3, the displacement of the right part of the EAS was different compared with the control. The OASI part was also in the right part of the EAS, so that is the most logical explanation for why that part differs.

4.3. Drawback analysis

There are some drawbacks of the displacement analysis that affect the results. Firstly, the analysis is mostly done on the middle slice of the EAS length and not on the whole 3D volume. In the controls, we saw only small differences in displacement over the length of the EAS, so this probably will not result in other results. In the OASI patients, this is not analysed yet; especially in the patient group, differences are expected due to damage in (a part of) the EAS. However, only the middle slices of the EAS already give other displacements in a patient than in control. Secondly, the displacements were calculated in the US coordinate system's x-, y- and z-direction. The position and orientation of the EAS differs between the different controls and patients and depends on the probe position during the TPUS assessment. Consequently, the movement of the EAS due to the PRM can also influence the displacements values in the other directions. Thirdly, the defined axis in the US-coordinate system does not correspond completely to the anatomical axis of the body due to the position and rotation of the probe during the TPUS assessment. The cranial direction defined in the US coordinate system is more in the direction between the anterior and cranial directions in the body. However, the cranial direction in the US coordinate system is more in the direction of the sphincter's length. These differences do not affect the displacement itself but the clinical interpretation of the displacement values in the x, y, and z-axis. Lastly, the EASs voxels makes one movement during contraction, but the displacements were analysed in each direction individually. The analysing per axis makes it more difficult to interpret how the whole sphincter moves because the colour bar axis also differs between the directions. However, due to the analysis per axis, the effect of the PRM is mainly seen in the x-direction, and it is easier to compare the displacements of the sphincter in the y-direction and z-direction, which the EAS mostly causes.

There are some limitations of the data used in this study. Firstly, the number of controls and patients is limited. However, there are already differences between the groups despite these low numbers, which is very promising. Secondly, the rest frame and the contraction frame are selected in the TPUS images. It is difficult to select the correct frame before contraction and the frame at the maximum contraction when there is less contraction. This selection can influence the results because the EAS displacement between these frames is calculated. Moreover, if a woman does not know how to contract her sphincter consciously, it does not immediately mean that the sphincter is not working since the EAS can also contract unconsciously. Lastly, it could be that the probe moved during the TPUS recording, but it was tried to keep the probe as steady as possible. Moving the probe during contraction also displaces the EAS in the recording, so some displacement could also be due to the probe movements and not the EAS contraction.

4.4. Future perspectives

This pilot study shows that it is technically feasible to segment the EAS manually and determine the 3D displacements. However, the software could still be optimised for the EAS. The chosen kernel size was based on another data set, and we saw a poorer tracking of the EAS with a larger contraction. The data of the other dataset consist of smaller voxel sizes, so optimising the kernel and template sizes on this data could give better results in tracking the EAS and displacement values of the EAS. To determine the necessity of changing these sizes, the EAS can also be segmented in the maximum contraction frame, and the Dice score and Haussdorf distance between the tracked and manually segmented EAS can be calculated. Based on these results can be determined if a change in kernel and template size is necessary. Further, this pilot study shows different displacements between controls and patients. However, the results are challenging to interpret, and improvements are needed to make an easier interpretation and comparison possible because that is necessary for clinical use. Therefore, expressing the EAS function as a value possible to calculate a strain is useful. At least two steps are necessary to investigate whether a strain could express the EAS function in one value. The first step is to change the US coordinate system into a coordinate system with one axis in the length of the anal canal and the other 2 in the anterior-posterior and left-right EAS parts. The displacement can then be calculated in this new coordinate system, resulting in the probe's angle having no influence on the displacements. The second step is that the displacement could also be calculated in a cylindrical coordinate system. The z value in the cylindrical coordinate system can correspond with the x-axis in the US-coordinate system. The r and theta can be determined in the yz-plane of the US coordinate system. This coordinate system gives more information about what happened in a circular structure because that is difficult to interpret in a cartesian coordinate system. To know if a strain calculation is a good step to express the EAS function in a value, it is important to see a gradient in the displacement values calculated in the cylindrical coordinate system, especially in the r and theta values because the z value is in the EAS length and is caused by the PRM. A gradient in these values means there will be a deformation of the EAS in that direction, resulting in the strain that can be used. If there is no gradient in the axis, it should be investigated whether the function can be expressed in another outcome measurement. That outcome measurement should then be compared to manometry measurements, because Jordan et al. [15] have studied that their protocol, including the manometry measurement, can help clinicians in their decision-making between vaginal delivery and caesarean. The manometry measurement was used to determine the function of that study. However, it is also important to realise that other pelvic floor muscles also influence the manometry measurements because an avulsion of the levator ani muscle is associated with a lower manometric squeeze pressure[23] possible that an avulsion of the levator ani muscle is also important information for the counselling. If it is possible to express the function of the EAS with 4D TPUS assessment, this tool could be used in the counselling of pregnant women with a previous OASI. However, also in women in the postpartum period with an

OASI during vaginal delivery, to determine the function as a preventive screening for the future and whether or not advising pelvic floor physical therapy.

5. Conclusion

In conclusion, the results of this pilot study are very positive and promising. It is technically feasible to segment and determine the 3D displacement of the EAS in 4D TPUS recordings, and there were different displacements between the controls and patients. The meaning of these differences in EAS function cannot be concluded yet.

References

[1] M. J. Heineman, "Obstetrie en Gynaecologie: de voortplanting van de mens," in *Obstetrie en Gynaecologie: de voortplanting van de mens*, J. L. H. Evers, Ed., 5th ed.Elsevier Maarssen, 2004, p. 654.

[2] J. L. Rasmussen and K. C. Ringsberg, "Being involved in an everlasting fight – a life with postnatal faecal incontinence. A qualitative study," *Scand J Caring Sci*, vol. 24, no. 1, pp. 108–115, Mar. 2010, doi: 10.1111/J.1471-6712.2009.00693.X.

[3] G. A. Santoro and A. H. Sultan, "Pelvic floor anatomy and imaging," *Semin Colon Rectal Surg*, vol. 27, no. 1, pp. 5–14, Mar. 2016, doi: 10.1053/J.SCRS.2015.12.003.

[4] A. Makol, M. Grovet, and W. E. Whitehead, "Fecal incontinence in women: Causes and treatment," *https://doi.org/10.1177/174550650800400501*, vol. 4, no. 5, Sep. 2020, doi: 10.1177/174550650800400501.

[5] W. E. Whitehead *et al.*, "Fecal Incontinence in U.S. Adults: Epidemiology and Risk Factors," *Gastroenterology*, vol. 137, no. 2, p. 512, 2009, doi: 10.1053/J.GASTRO.2009.04.054.

[6] E. M. J. Bols, E. J. M. Hendriks, B. C. M. Berghmans, C. G. M. I. Baeten, J. G. Nijhuis, and R. A. De Bie, "A systematic review of etiological factors for postpartum fecal incontinence," *Acta Obstet Gynecol Scand*, vol. 89, no. 3, pp. 302–314, Mar. 2010, doi: 10.3109/00016340903576004.

[7] D. Borello-France *et al.*, "Fecal and urinary incontinence in primiparous women," *Obstetrics and Gynecology*, vol. 108, no. 4, pp. 863–872, Sep. 2006, doi: 10.1097/01.AOG.0000232504.32589.3B.

[8] M. M. Soerensen, S. Buntzen, K. M. Bek, and S. Laurberg, "Complete obstetric anal sphincter tear and risk of long-term fecal incontinence: A cohort study," *Dis Colon Rectum*, vol. 56, no. 8, pp. 992–1001, Aug. 2013, doi: 10.1097/DCR.0B013E318299C209.

[9] A. H. Sultan, "Editorial: Obstetrical perineal injury and anal incontinence," *Clin Risk*, vol. 5, no. 6, pp. 193–196, Aug. 1999, doi: 10.1177/135626229900500601.

[10] "The Management of Third-and Fourth-Degree Perineal Tears Green-top Guideline No. 29." Royal College of Obstetricians & Gynaecologists, Jun. 2015.

[11] A. H. Sultan, R. Thakar, and D. E. Fenner, *Perineal and Anal Sphincter Trauma*. Springer London, 2007. doi: 10.1007/978-1-84628-503-5.

[12] Perined, "Perined, Utrecht, 2022." https://www.peristat.nl/ (accessed Nov. 09, 2022).

[13] I. E. K. Nilsson, S. Åkervall, M. Molin, I. Milsom, and M. Gyhagen, “Symptoms of fecal incontinence two decades after no, one, or two obstetrical anal sphincter injuries,” *Am J Obstet Gynecol*, vol. 224, no. 3, pp. 276.e1-276.e23, Mar. 2021, doi: 10.1016/J.AJOG.2020.08.051.

[14] K. Veuger, A. Veenstra van Nieuwenhoven, A. Goos, and L. van Genugten, “Protocol ZGT: Totaal ruptuur tijdens baring of in de voorgeschiedenis.”

[15] P. A. Jordan, M. Naidu, R. Thakar, and A. H. Sultan, “Effect of subsequent vaginal delivery on bowel symptoms and anorectal function in women who sustained a previous obstetric anal sphincter injury,” *Int Urogynecol J*, vol. 29, no. 11, pp. 1579–1588, Nov. 2018, doi: 10.1007/s00192-018-3601-y.

[16] K. Hotta *et al.*, “Diagnosis of anal sphincter defects by three-dimensional transperineal ultrasound in women with anal incontinence,” *Journal of Medical Ultrasonics*, vol. 39, no. 4, pp. 241–247, Oct. 2012, doi: 10.1007/S10396-012-0369-4.

[17] J. H. Lee, D. H. Pretorius, M. Weinstein, N. M. Guaderrama, C. W. Nager, and R. K. Mittal, “Transperineal three-dimensional ultrasound in evaluating anal sphincter muscles,” *Ultrasound in Obstetrics and Gynecology*, vol. 30, no. 2, pp. 201–209, Aug. 2007, doi: 10.1002/uog.4057.

[18] S. Das *et al.*, “3D Ultrasound Strain Imaging of Puborectalis Muscle,” *Ultrasound Med Biol*, vol. 47, no. 3, pp. 569–581, Mar. 2021, doi: 10.1016/J.ULTRASMEDBIO.2020.11.016.

[19] M. Hölscher, C. Gräf, A. L. Stickelmann, E. Stickeler, and L. Najjari, “Perianal ultrasound (PAUS): visualization of sphincter muscles and comparison with digital-rectal examination (DRE) in females,” *BMC Womens Health*, vol. 21, no. 1, pp. 1–13, Dec. 2021, doi: 10.1186/S12905-021-01387-1/TABLES/8.

[20] J. H. Lee, D. H. Pretorius, M. Weinstein, N. M. Guaderrama, C. W. Nager, and R. K. Mittal, “Transperineal three-dimensional ultrasound in evaluating anal sphincter muscles,” *Ultrasound in Obstetrics and Gynecology*, vol. 30, no. 2, pp. 201–209, Aug. 2007, doi: 10.1002/UOG.4057.

[21] H. P. Dietz, M. Kreft, N. Subramaniam, and K. Robledo, “Location of obstetric anal sphincter injury scars on translabial tomographic ultrasound,” *Ultrasound in Obstetrics & Gynecology*, vol. 58, no. 4, pp. 630–633, Oct. 2021, doi: 10.1002/UOG.23719.

[22] J. Stroker, S. A. Taylor, and J. O. L. DeLancey, *Medical Radiology: Imaging Pelvic Floor Disorders*, 2nd revised. 2008. doi: 10.1007 / 978-3-540-71968-7.

[23] M. A. Guedea, J. L. A. Zambrano, J. B. Fons, L. J. Viana, B. O. Linaje, and J. Á. M. Milio, “Alteration of anal sphincter function in patients with levator avulsion: observational study,” *Int Urogynecol J Pelvic Floor Dysfunct*, vol. 26, no. 7, pp. 985–990, Jul. 2015, doi: 10.1007/S00192-014-2623-3.

[24] H. P. DIETZ, “Pelvic Floor Ultrasound: A Review,” *Clin Obstet Gynecol*, vol. 60, no. 1, pp. 58–81, Mar. 2017, doi: 10.1097/GRF.0000000000000264.

Appendices

Appendix A: Anatomical background information of the EAS

In women is the anteriorly part of the EAS shorter approximately 1.5 cm (in men approximately 2.7 cm). The lateral part is approximately 2.7 cm. The EAS has a thickness of approximately 4 mm.

The EAS consist of three parts (Figure 1):

- Deep part:
  - circular muscle fibers.
  - Blends with puborectalis part of levator ani (posteriorly and laterally).
- Superficial part:
  - Elliptical muscle fibers
  - Attaches from the tip of the coccyx posteriorly to the perineal body anteriorly
  - Only part of the sphincter with bone attachment
- Subcutaneous part:
  - Circular muscle fibers
  - Lower ends curve inwards, lying below the end of the internal sphincter

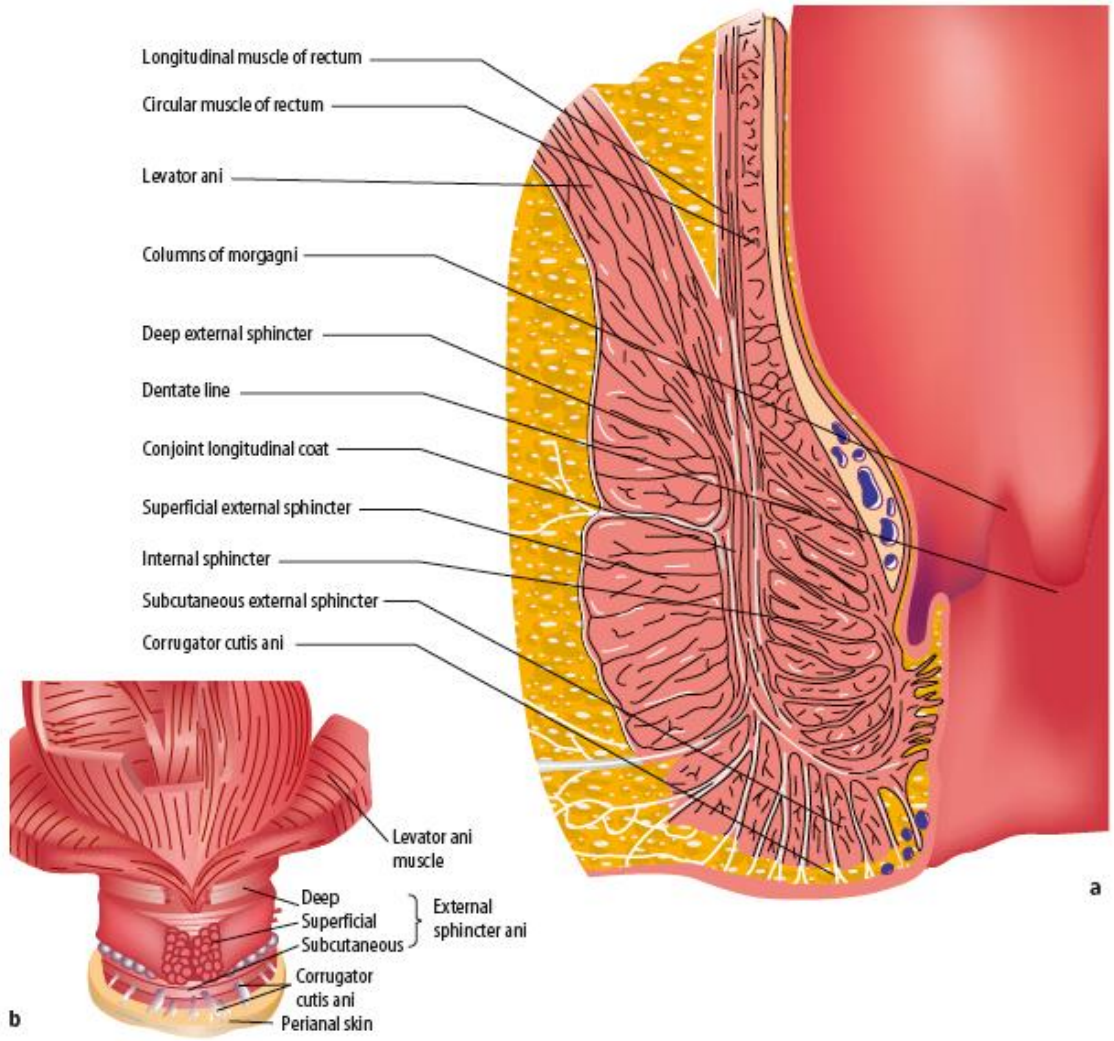

Figure 1. Anatomical view of the EAS and the different parts. a. coronal section of the anorectum. b. Anal sphincter and levator ani muscles.

Figures 2 and 3 show more information about the surrounding muscles of the pelvic floor and the attachment of the EAS. Figure 4 shows the anatomical location of the PRM and anal sphincter in a sagittal view of the pelvis.

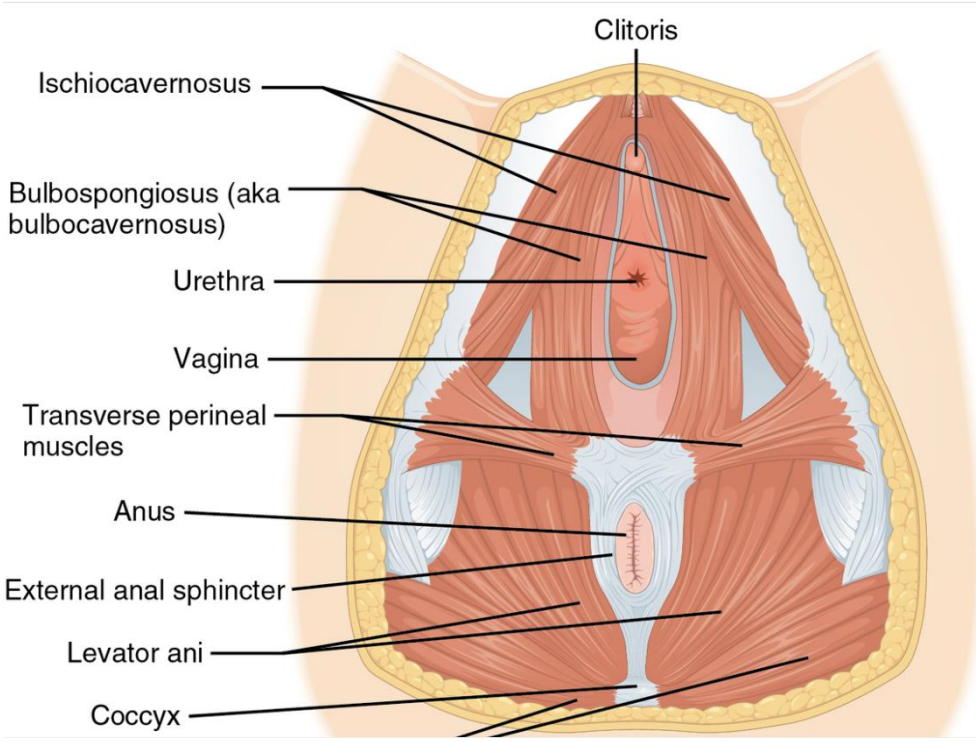

Figure 2. Overview of the different pelvic floor muscles and the attachment of the EAS with that muscles.

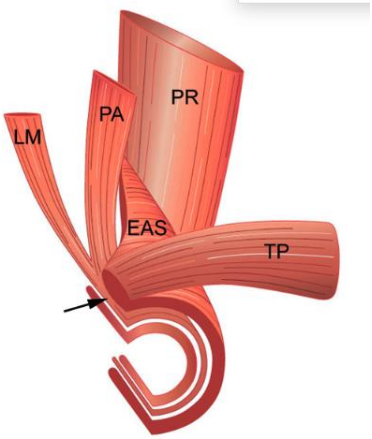

Figure 3. The tranverse perineii(TP) is seen to fuse with the EAS. The puborectalis (PR) forms a sling around the EAS.

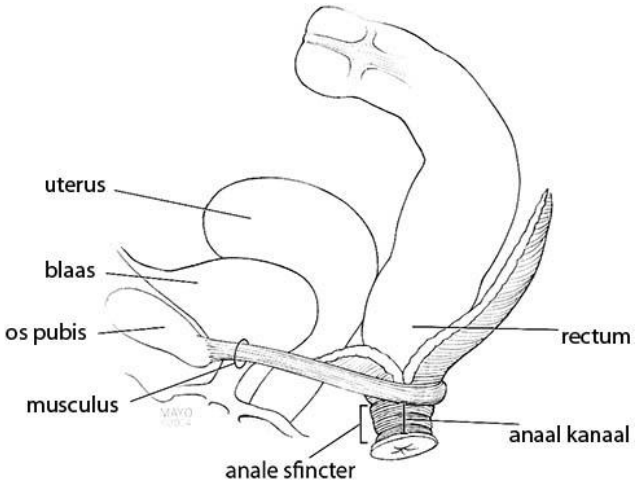

Figure 4. An overview of the pelvic structures and the PRM (musculus) and the anal sphincter.

Appendix B: Segmentation results of the controls

Control 1

3D Segmentation

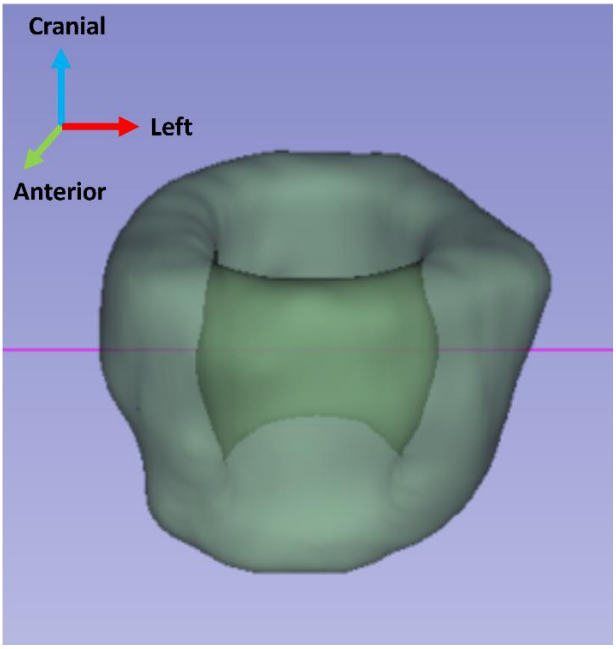

Transversal view

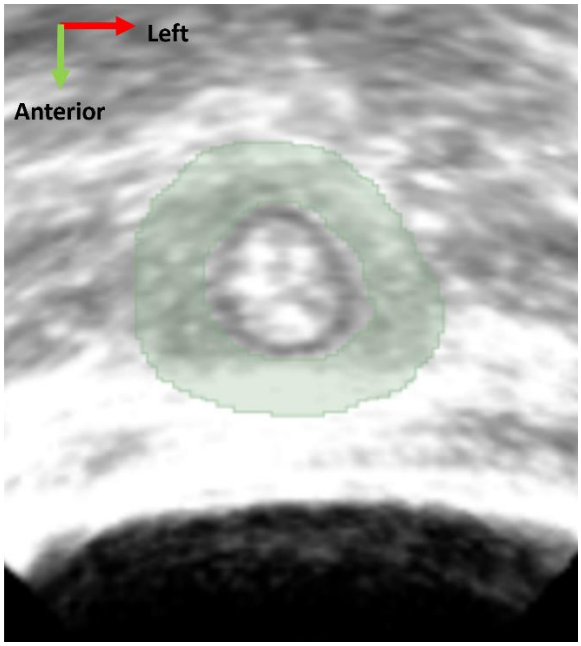

Sagittal view

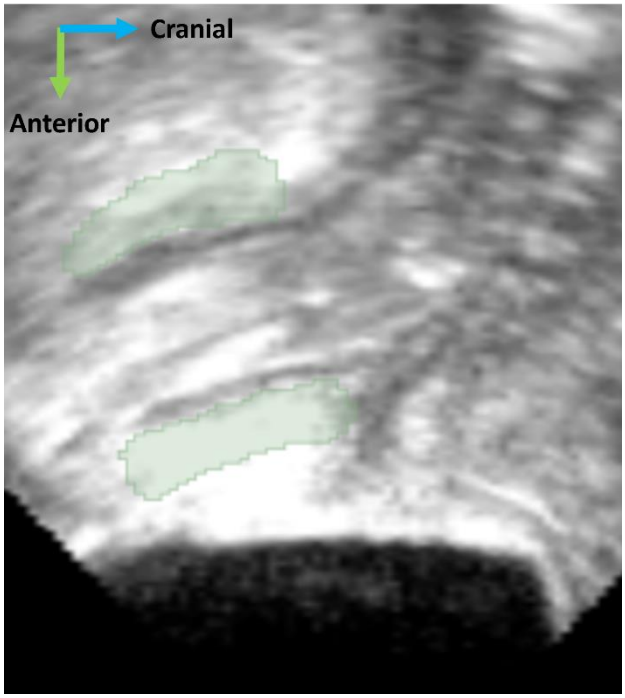

Coronal view

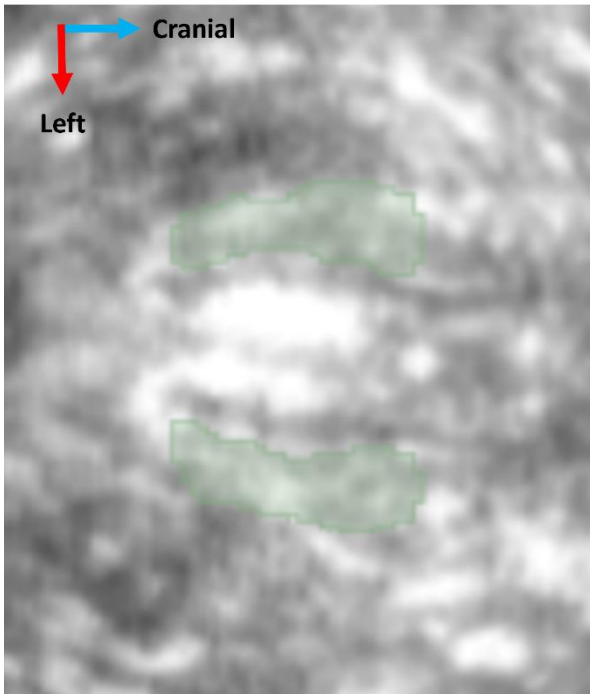

Control 2

3D Segmentation

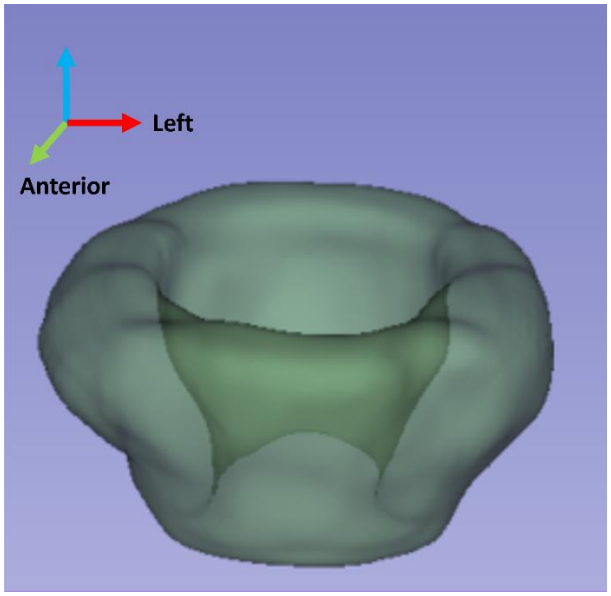

Transversal view

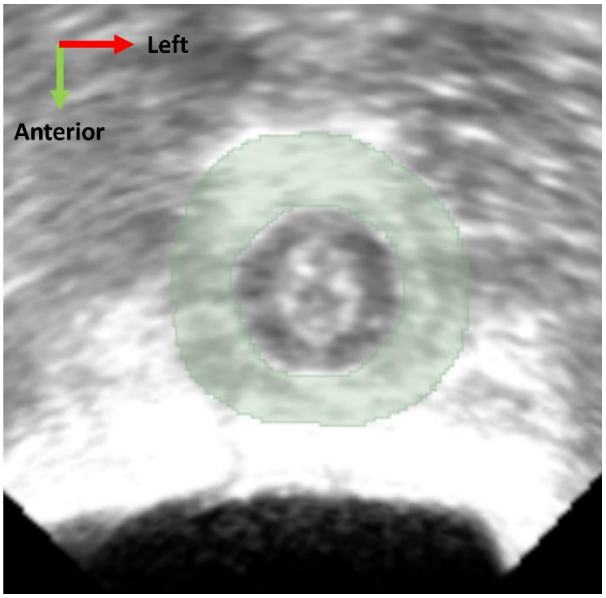

Sagittal view

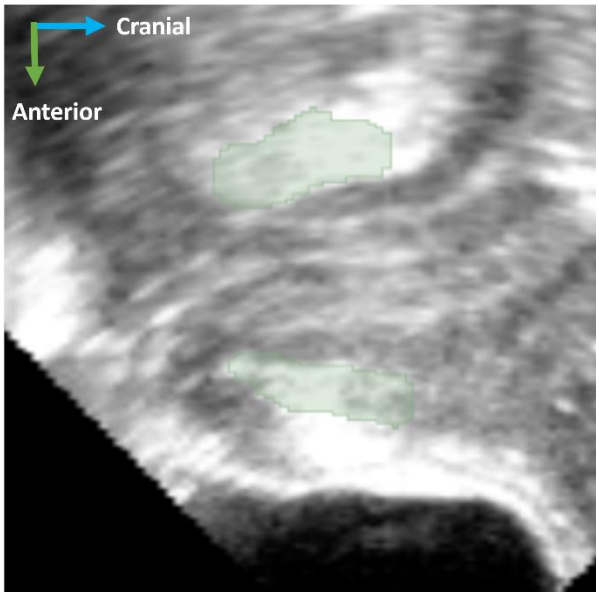

Coronal view

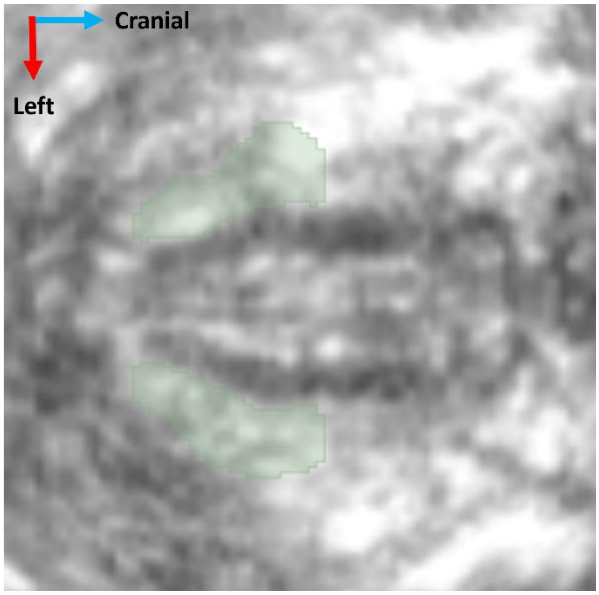

Control 3

3D Segmentation

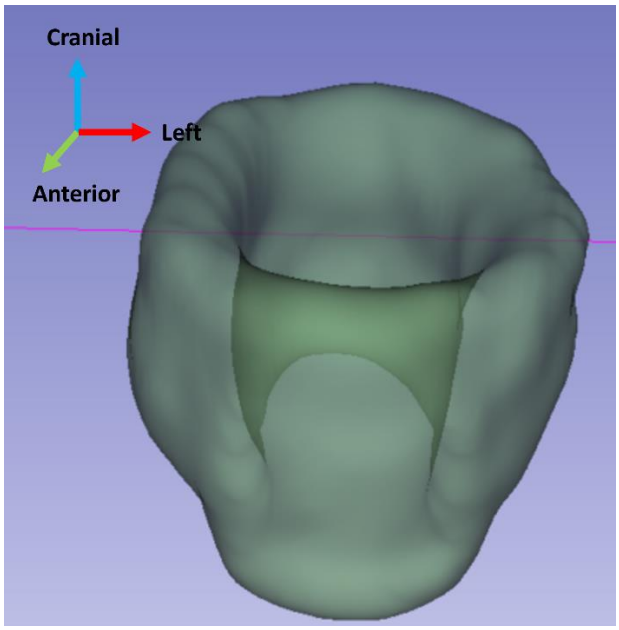

Transversal view

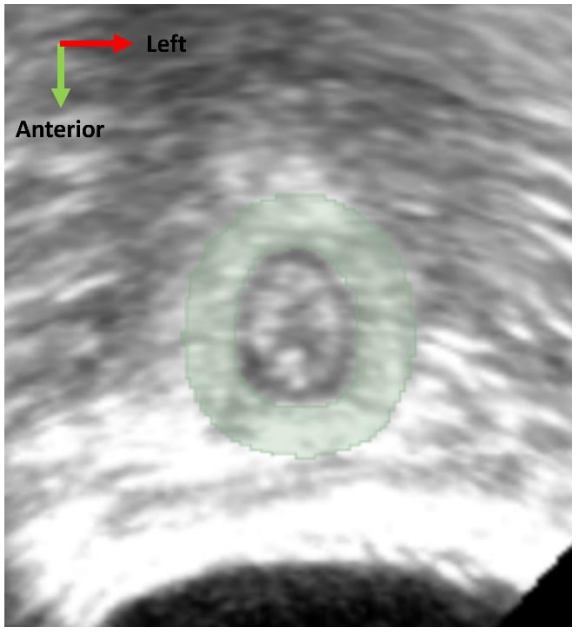

Sagittal view

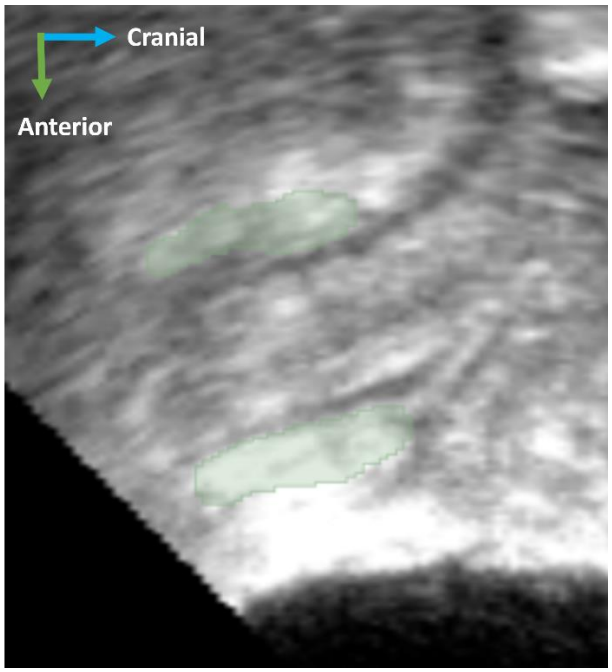

Coronal view

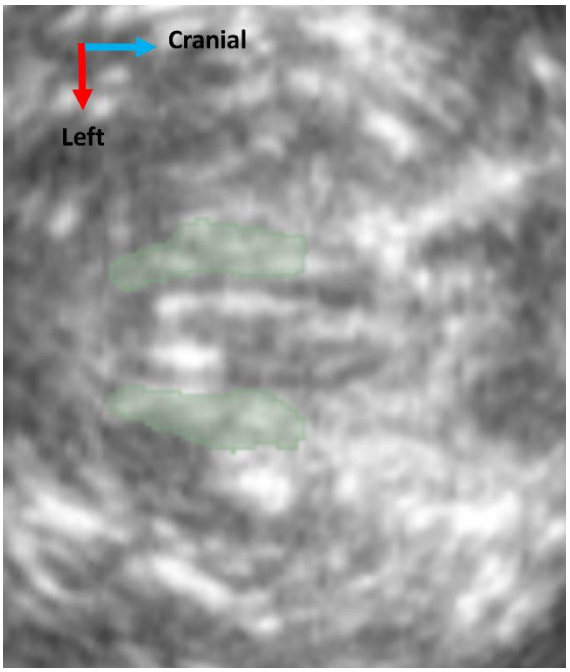

Control 4

3D Segmentation

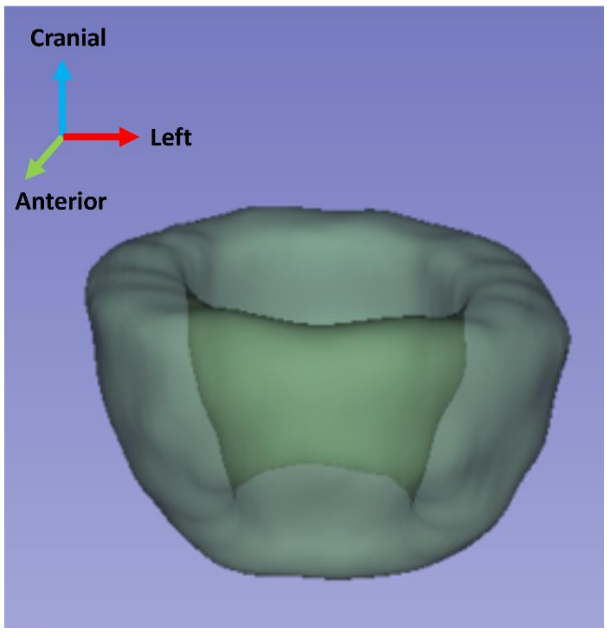

Transversal view

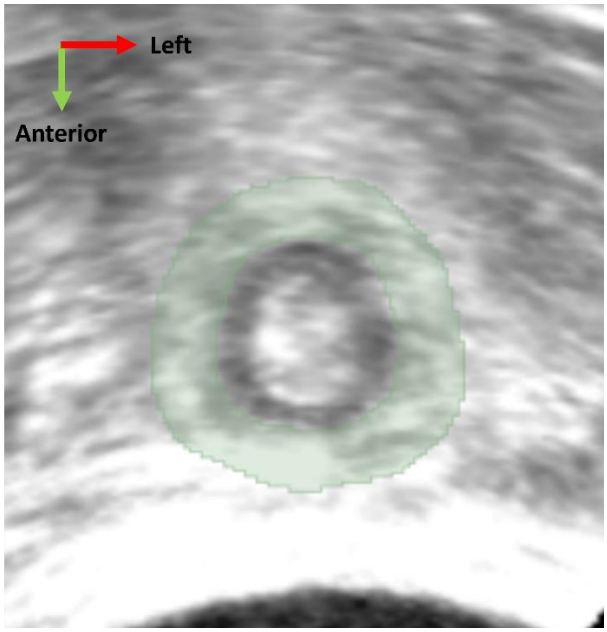

Sagittal view

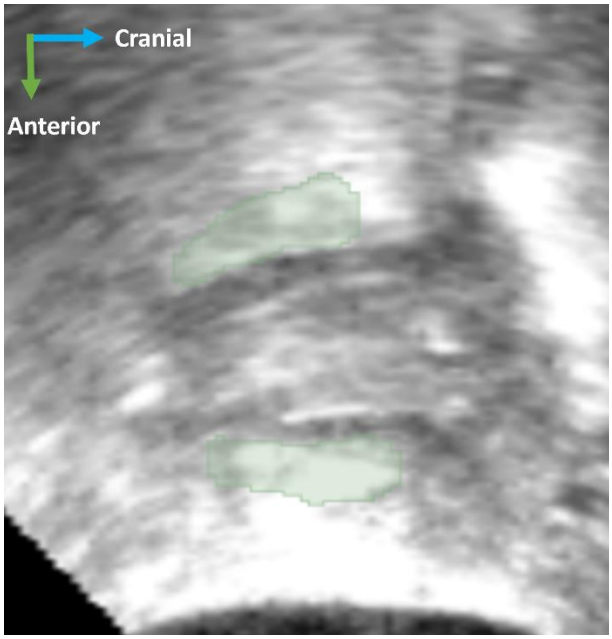

Coronal view

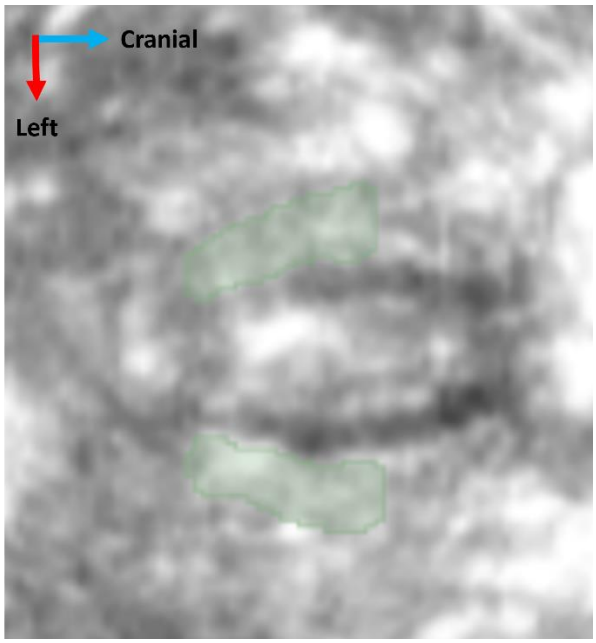

Control 5

3D Segmentation

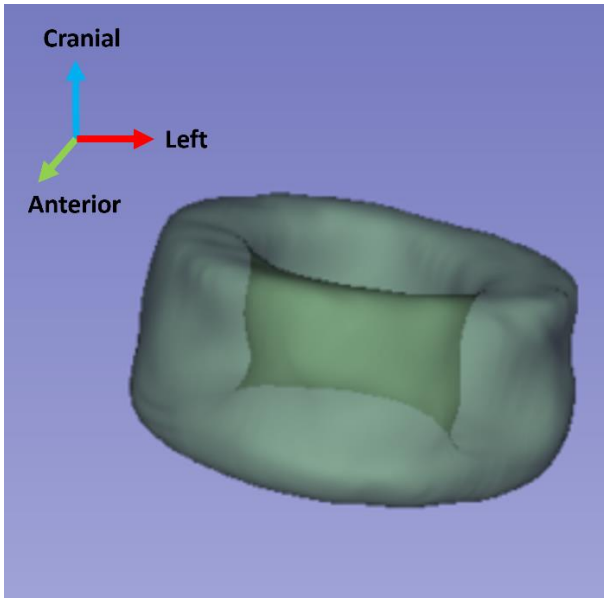

Transversal view

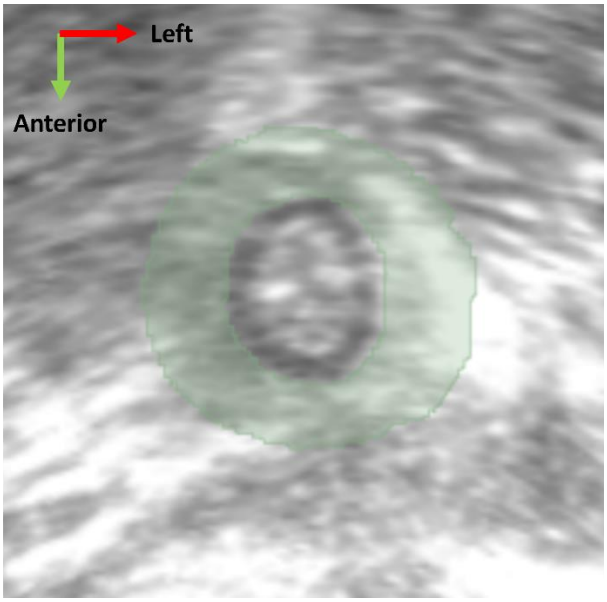

Sagittal view

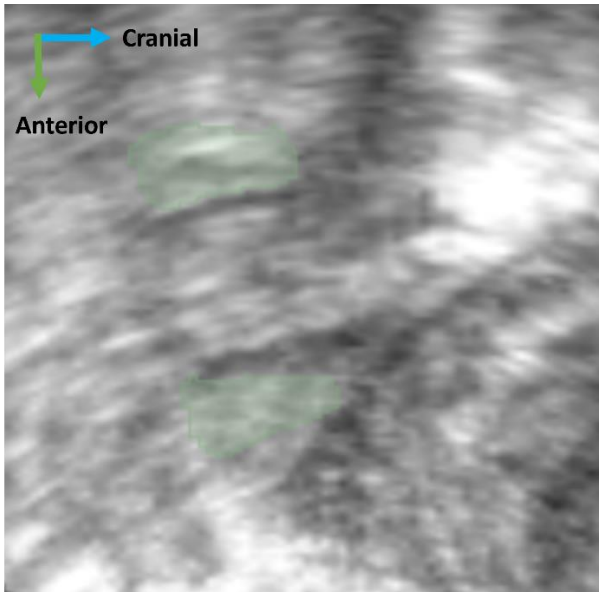

Coronal view

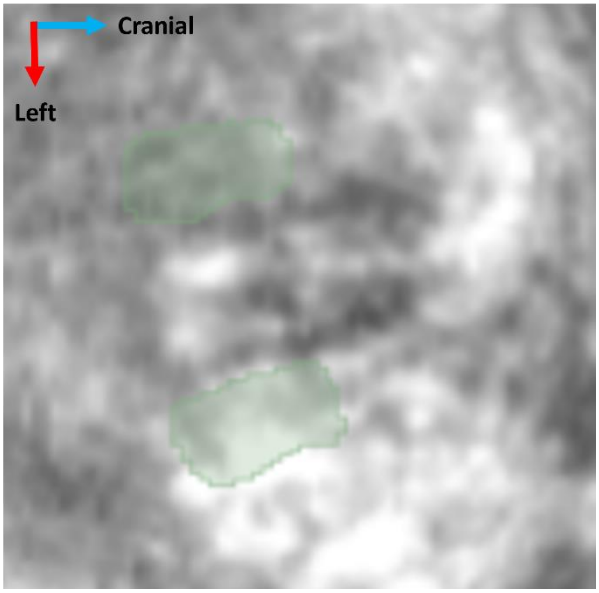

Appendix C: Segmentation results of the patients

Patient 1

3D Segmentation

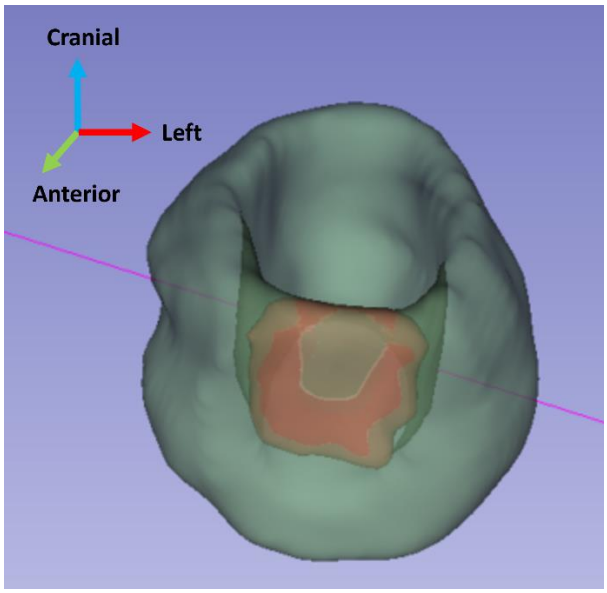

Transversal view

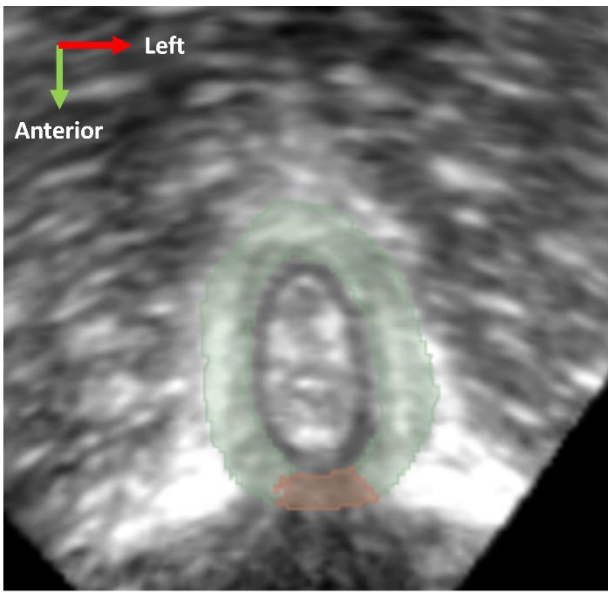

Sagittal view

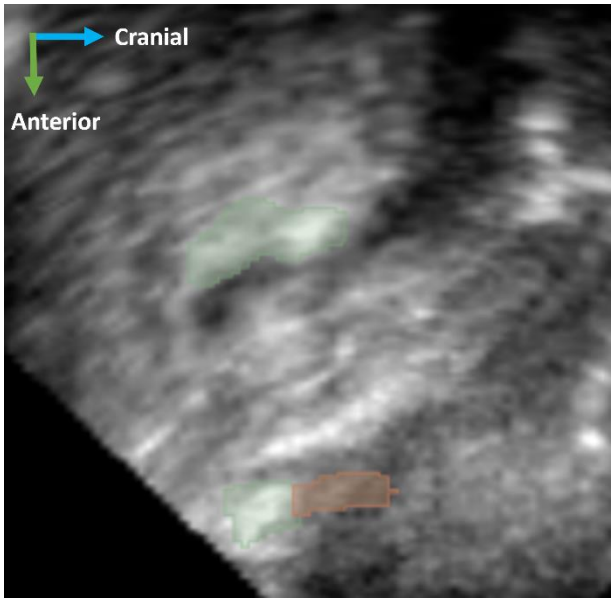

Coronal view

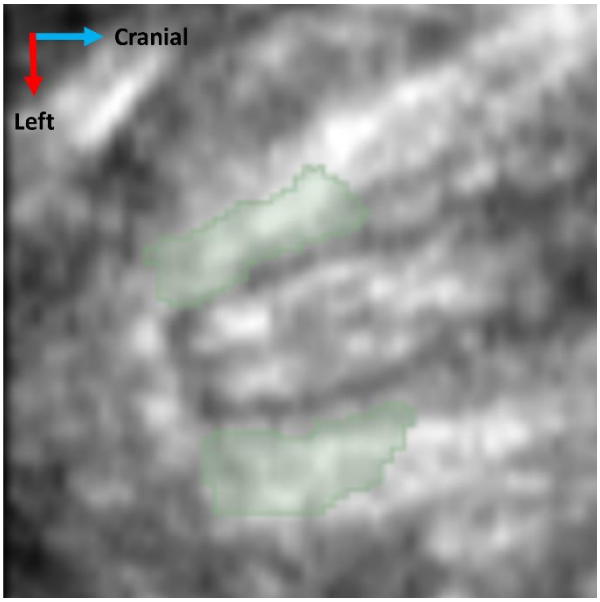

Patient 2

3D Segmentation

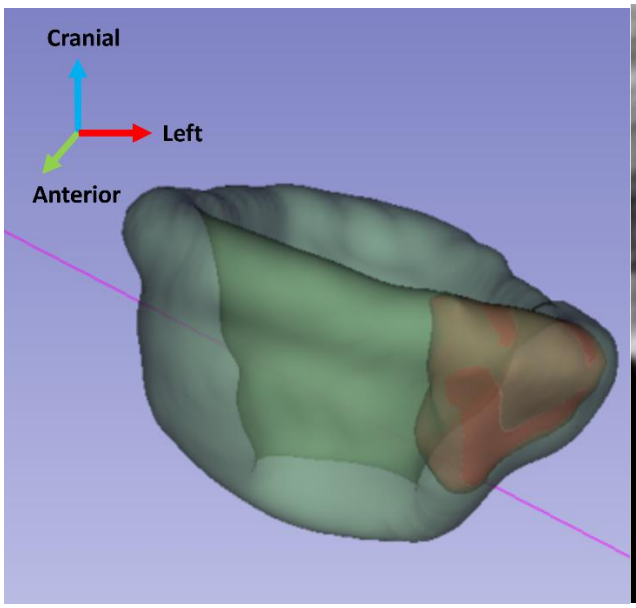

Transversal view

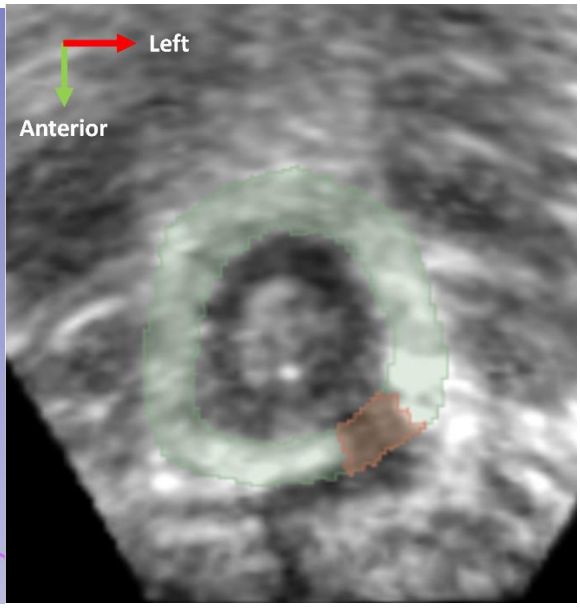

Sagittal view

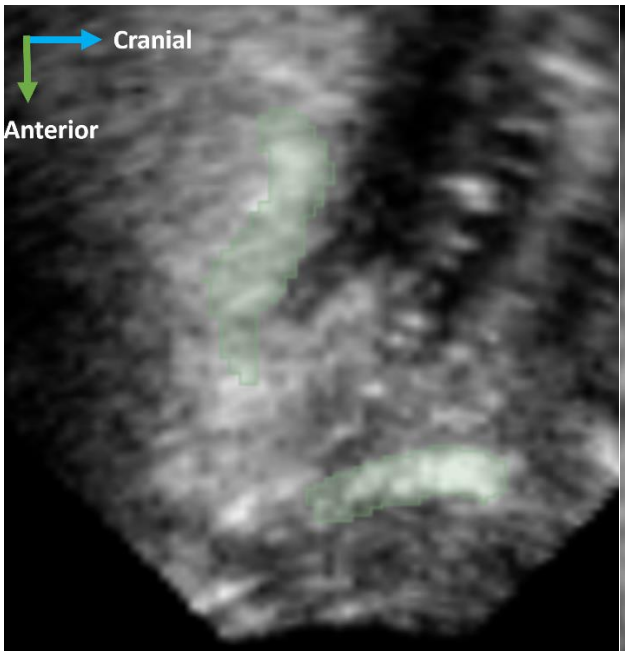

Coronal view

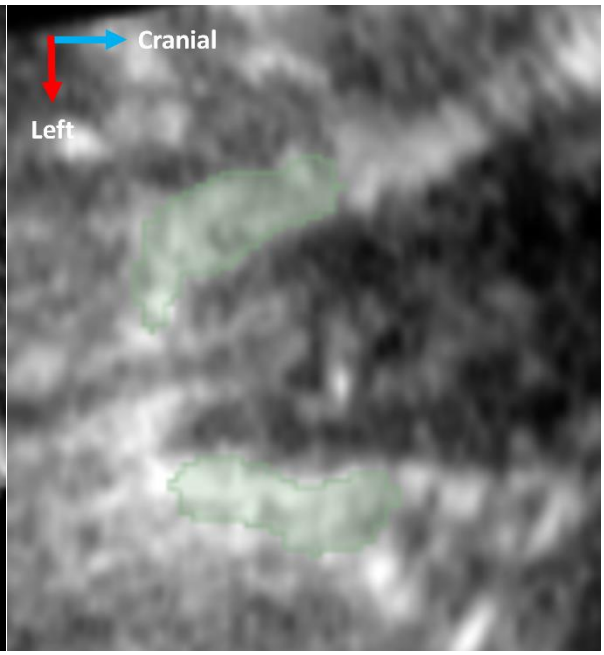

Patient 3

3D Segmentation

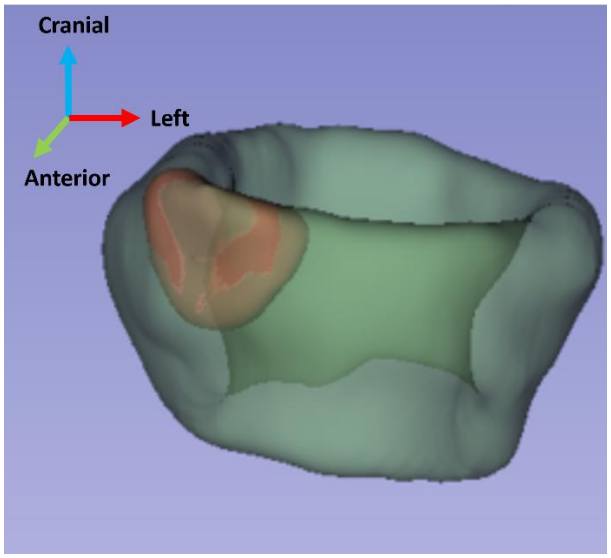

Transversal view

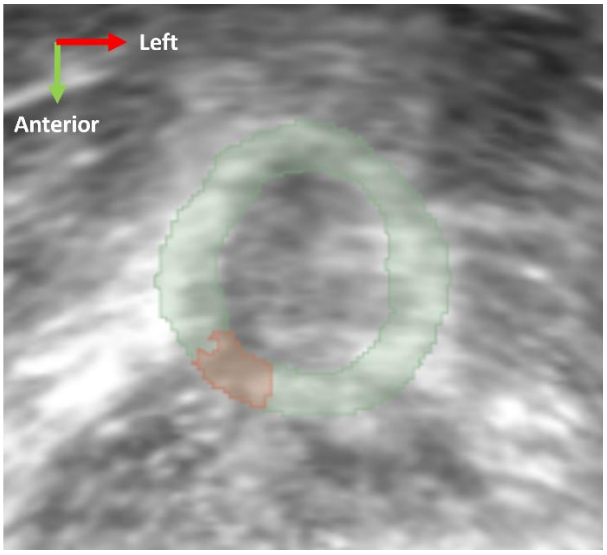

Sagittal view

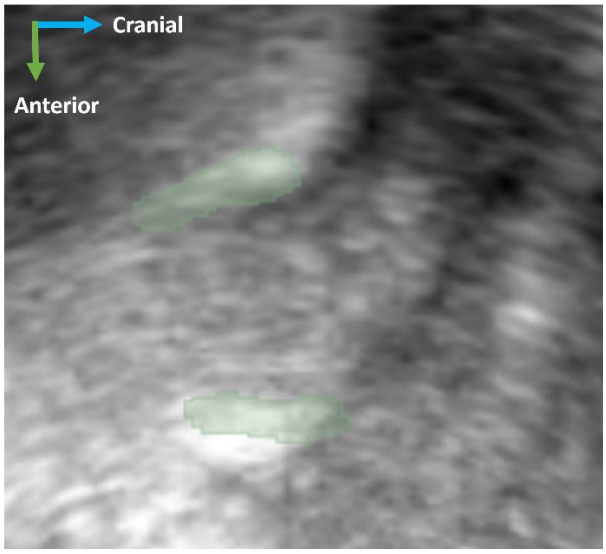

Coronal view

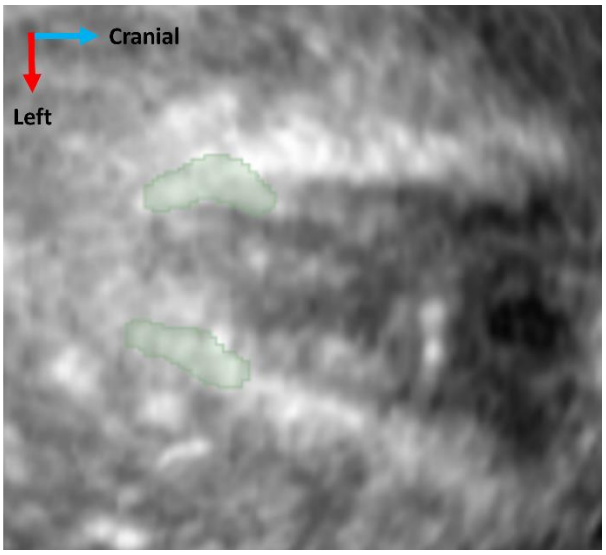

Patient 4

3D Segmentation

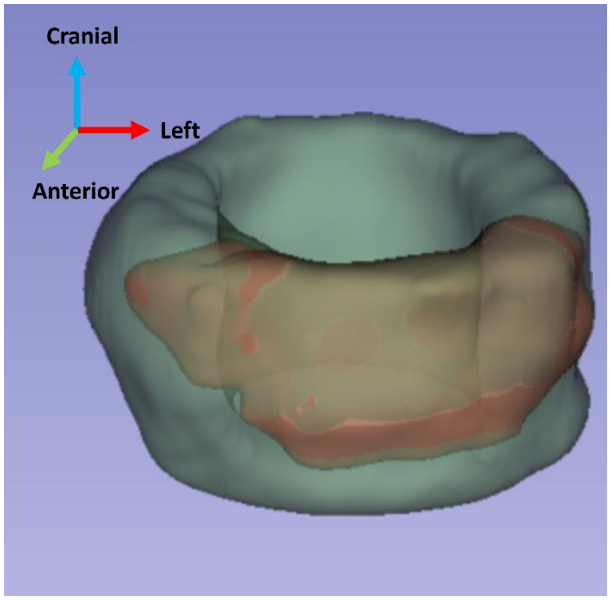

Transversal view

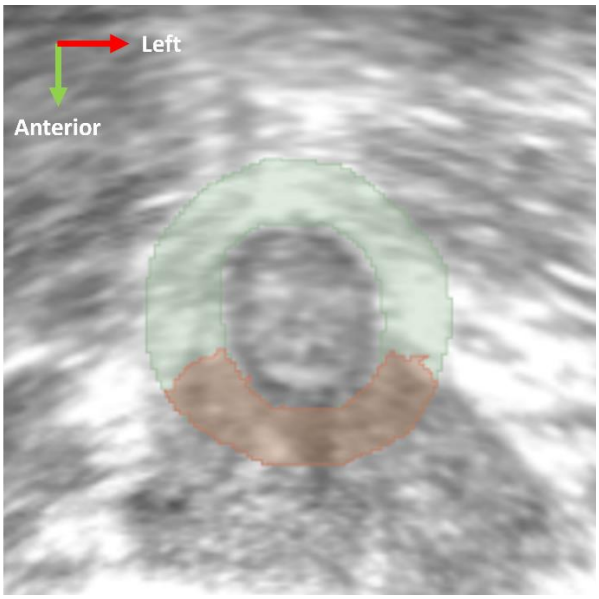

Sagittal view

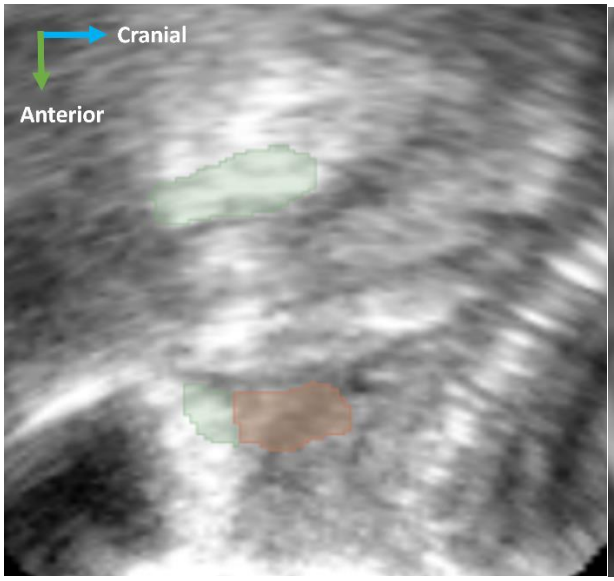

Coronal view

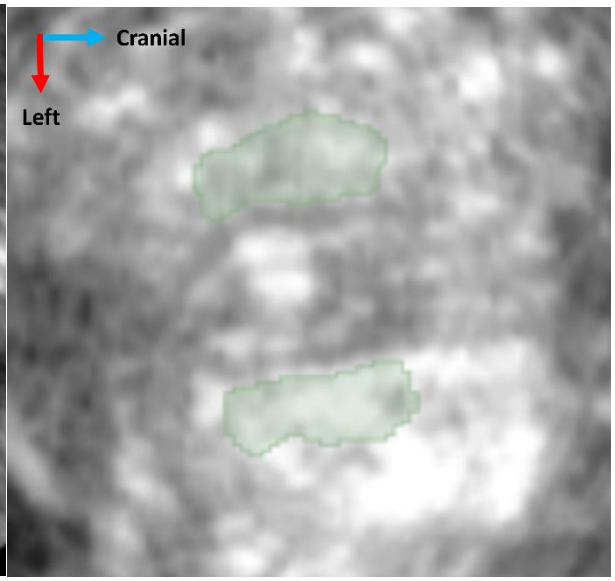

Patient 5

3D Segmentation

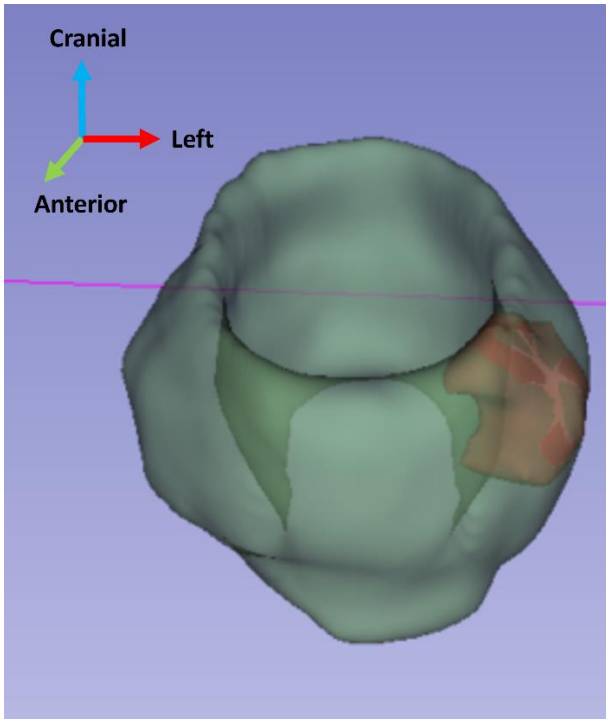

Transversal view

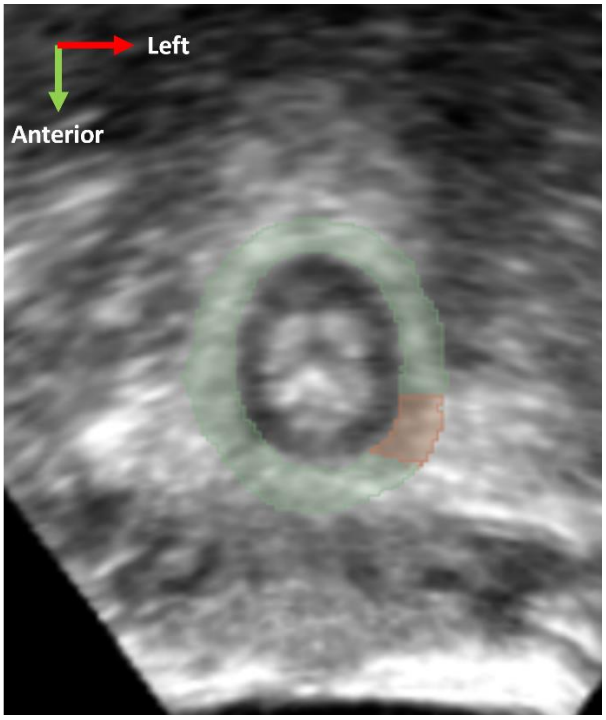

Sagittal view

Coronal view

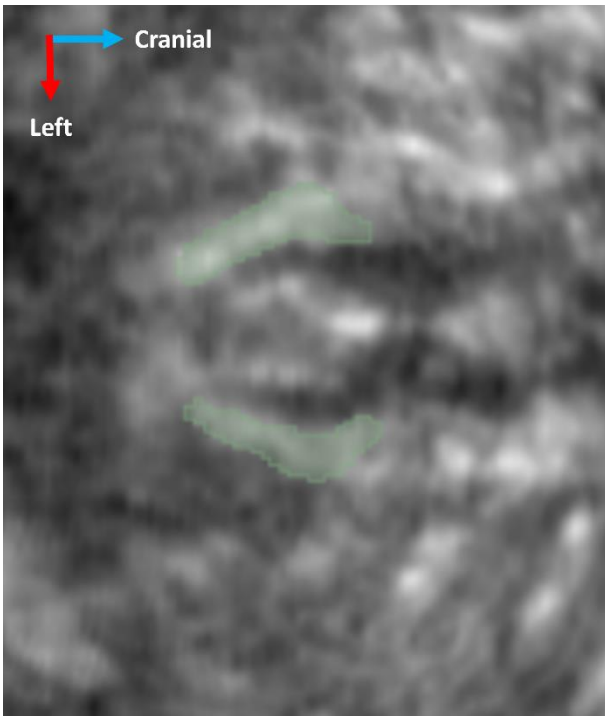

Appendix D: Displacement figures of the controls

Control 1

Displacement x-direction

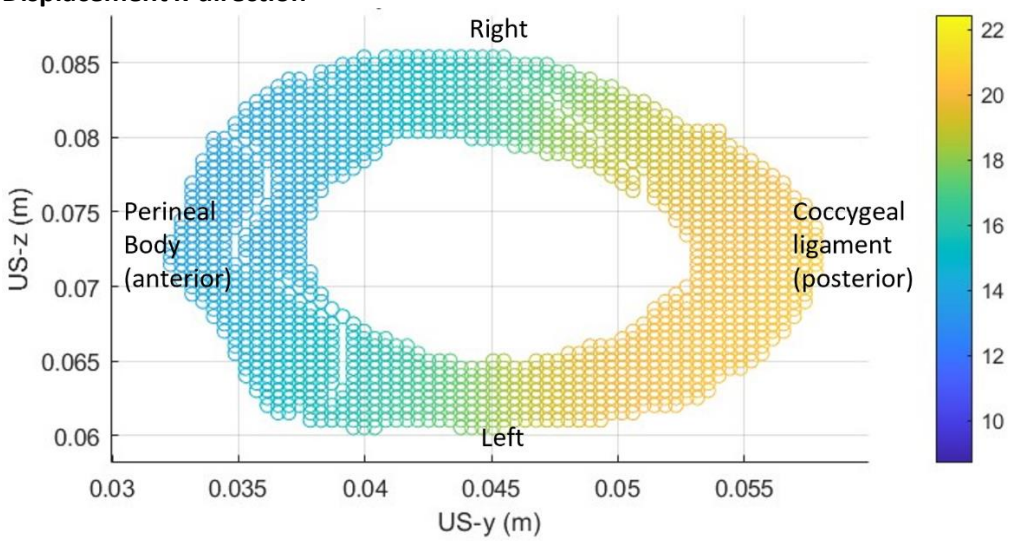

Displacement y-direction

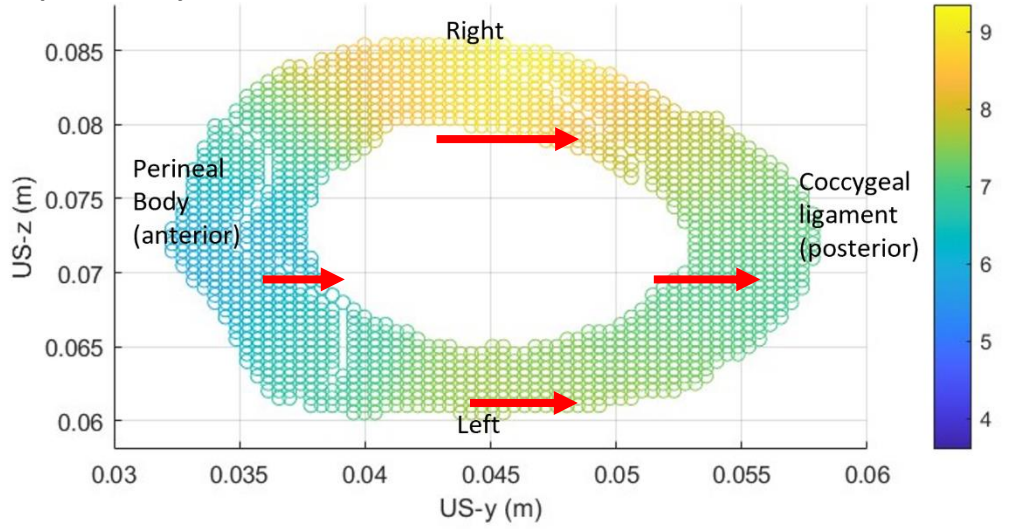

Displacement z-direction

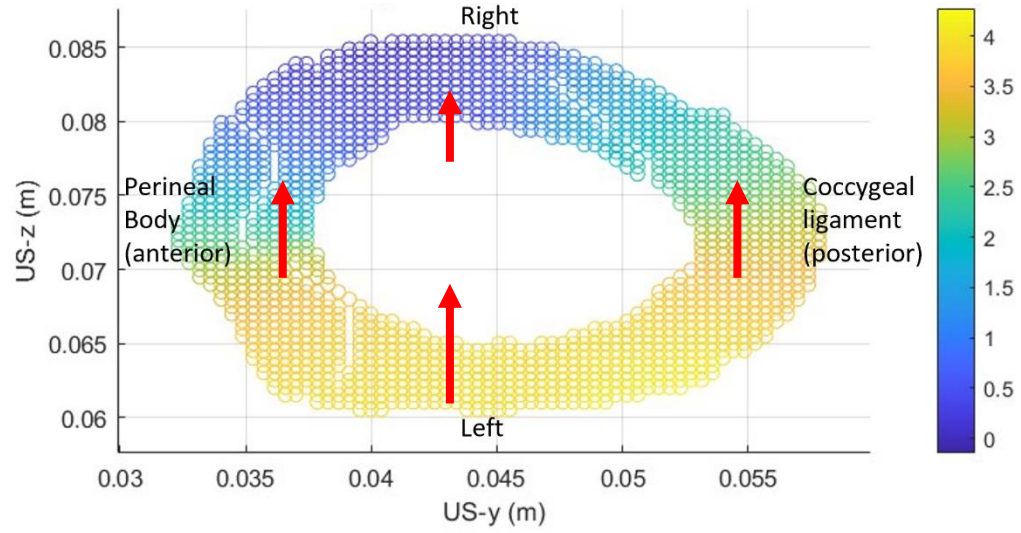

Control 2

Displacement x-direction

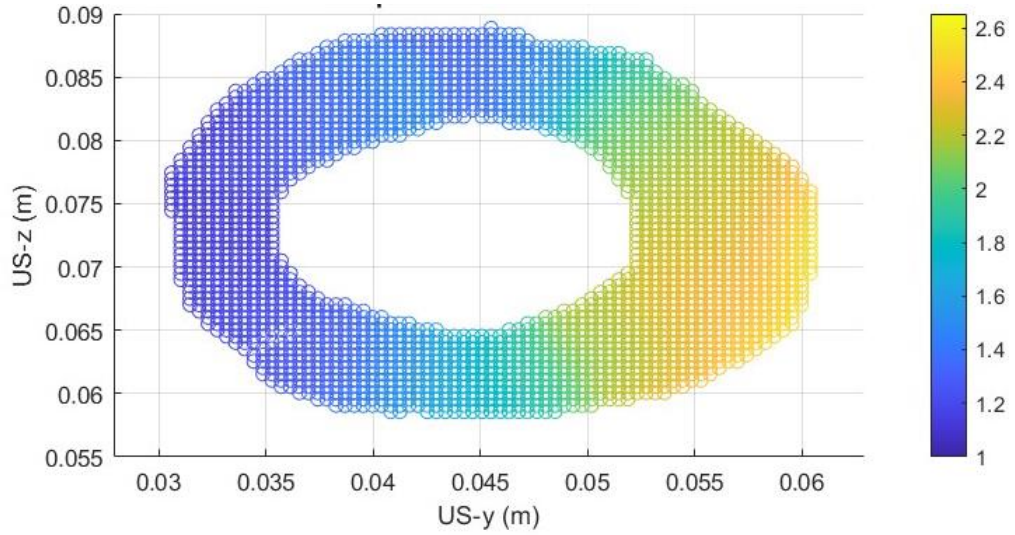

Displacement y-direction

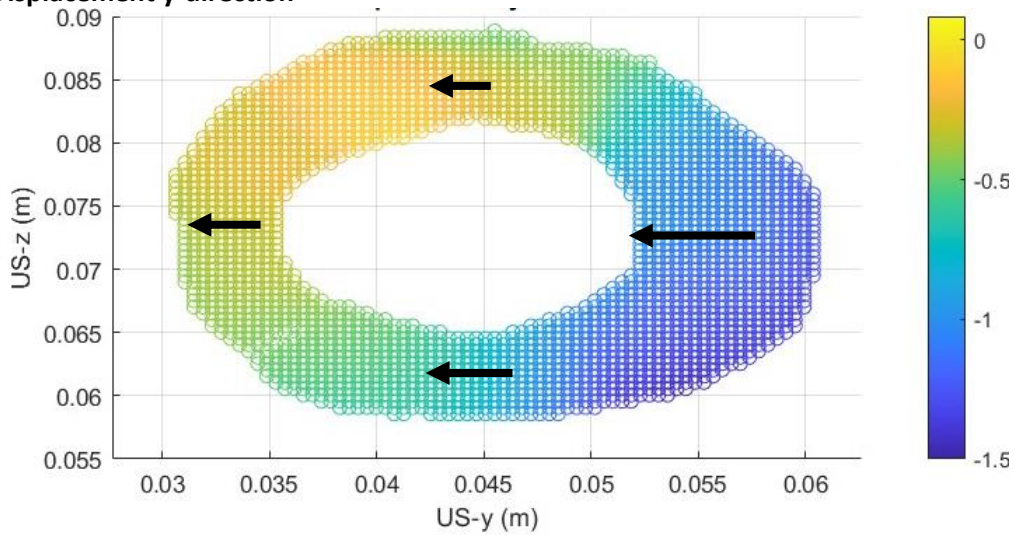

Displacement z-direction

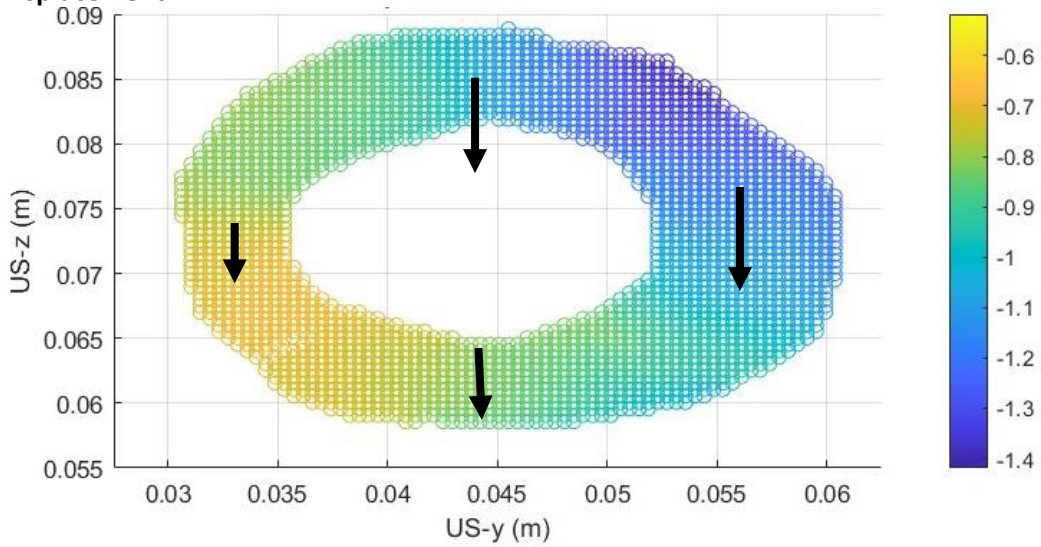

Control 3

Displacement x-direction

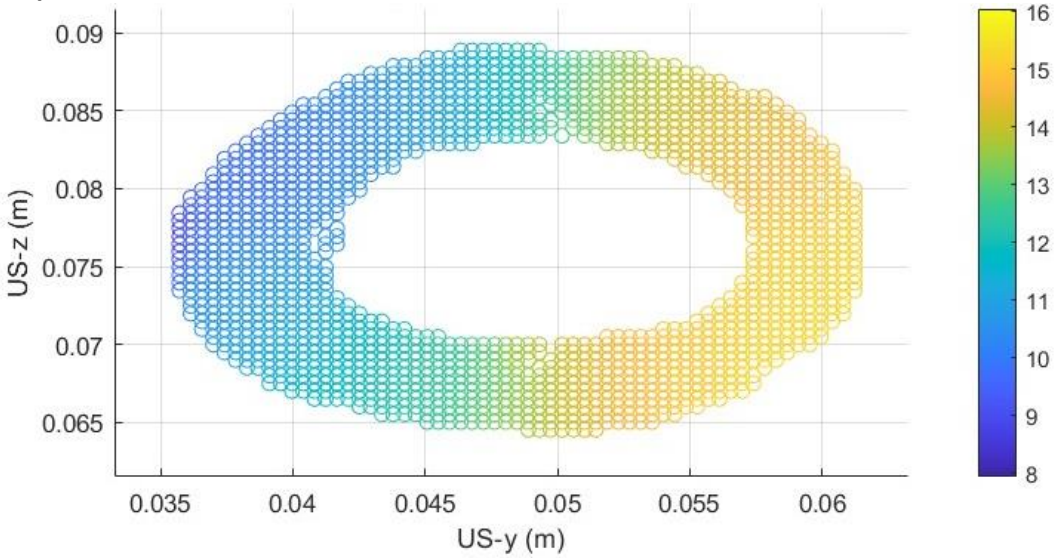

Displacement y-direction

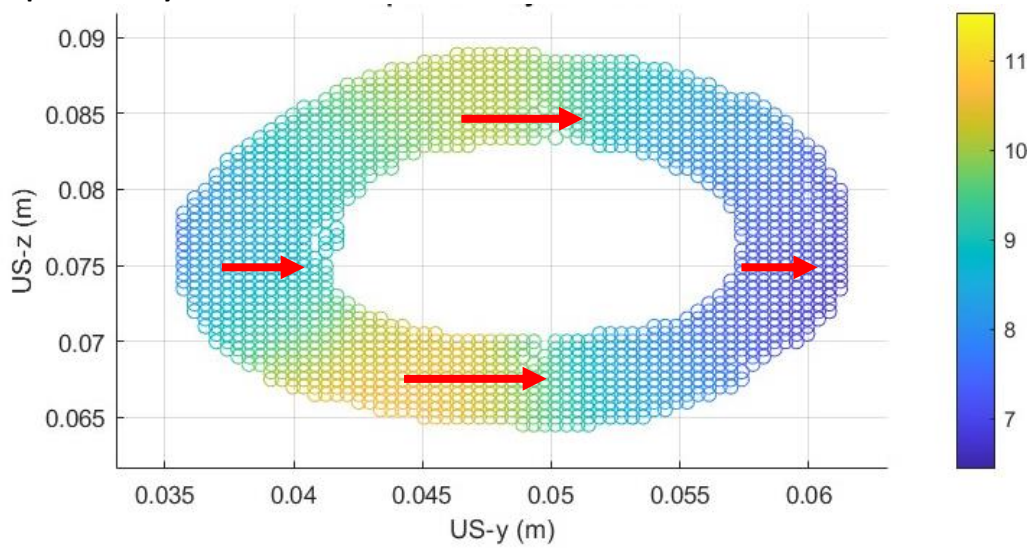

Displacement z-direction

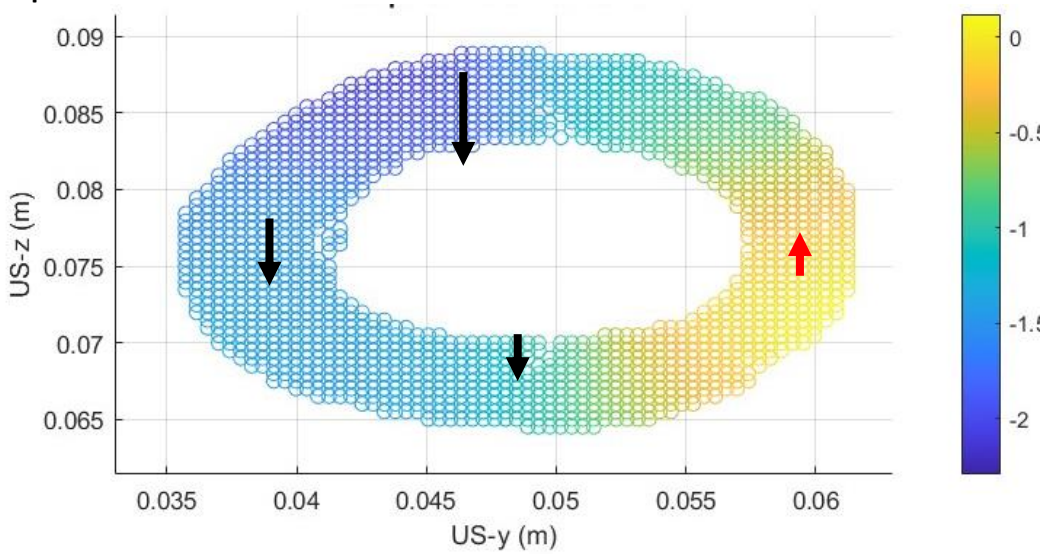

Control 4

Displacement x-direction

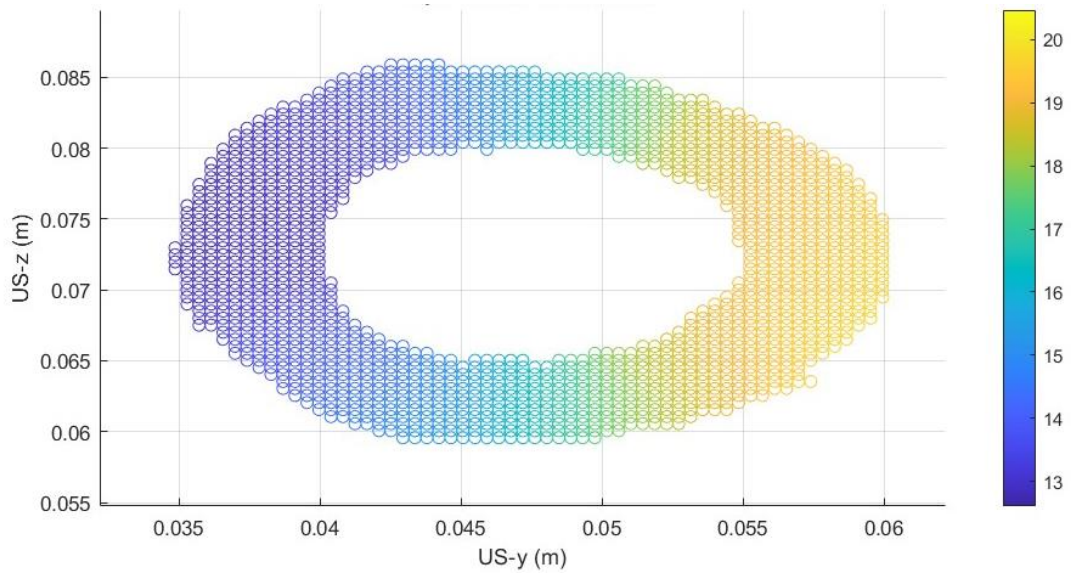

Displacement y-direction

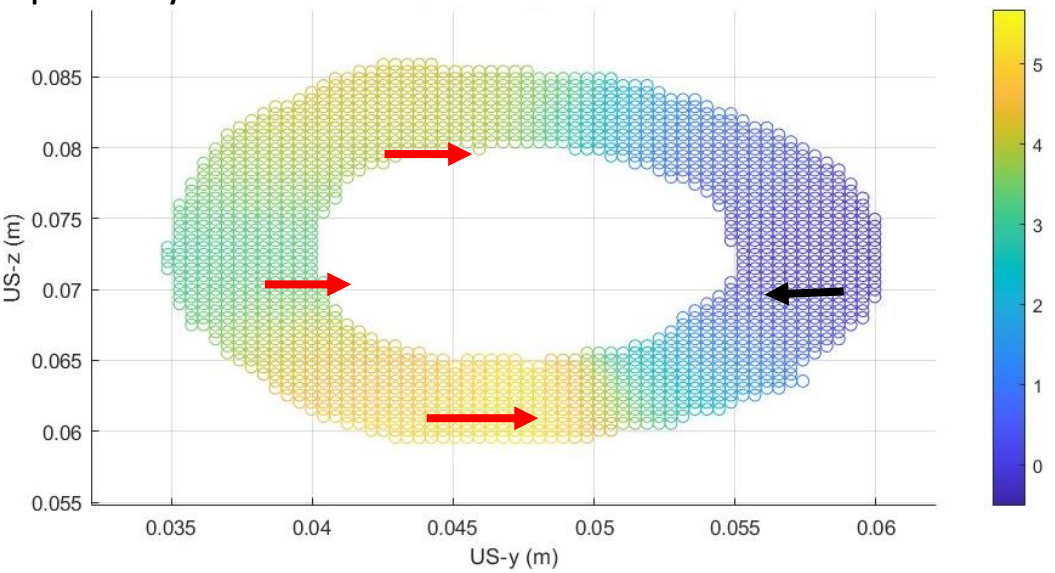

Displacement **z-direction**

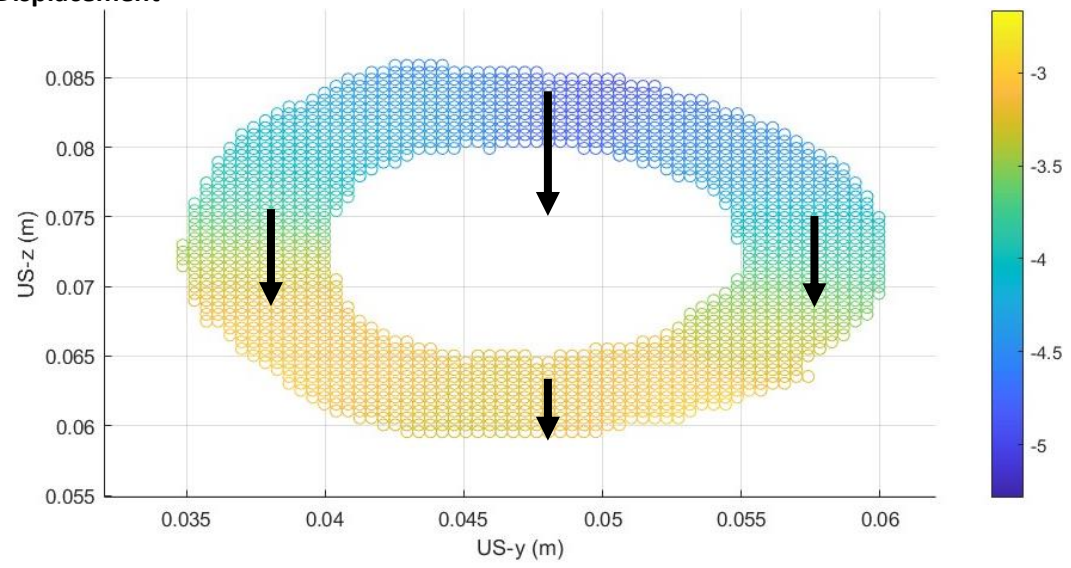

Control 5

Displacement x-direction

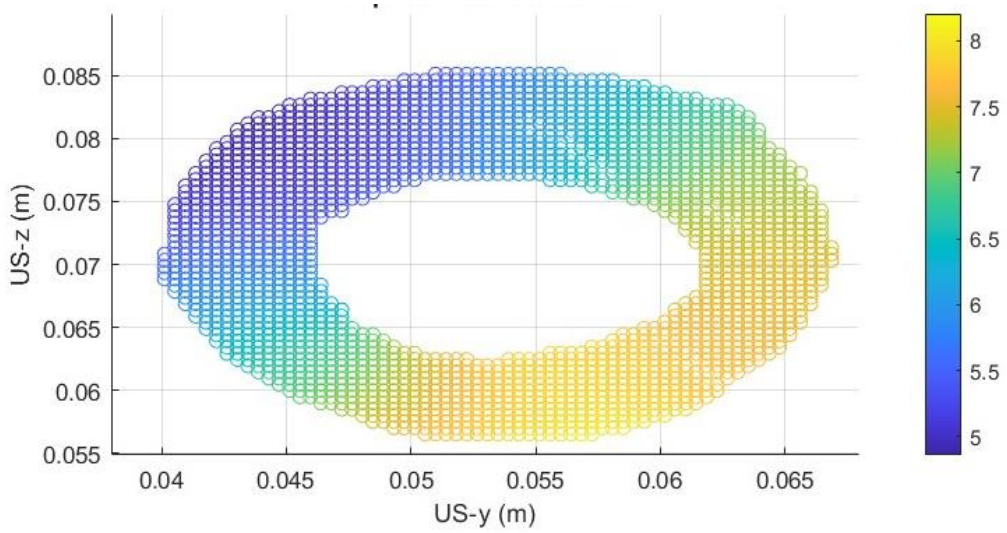

Displacement y-direction

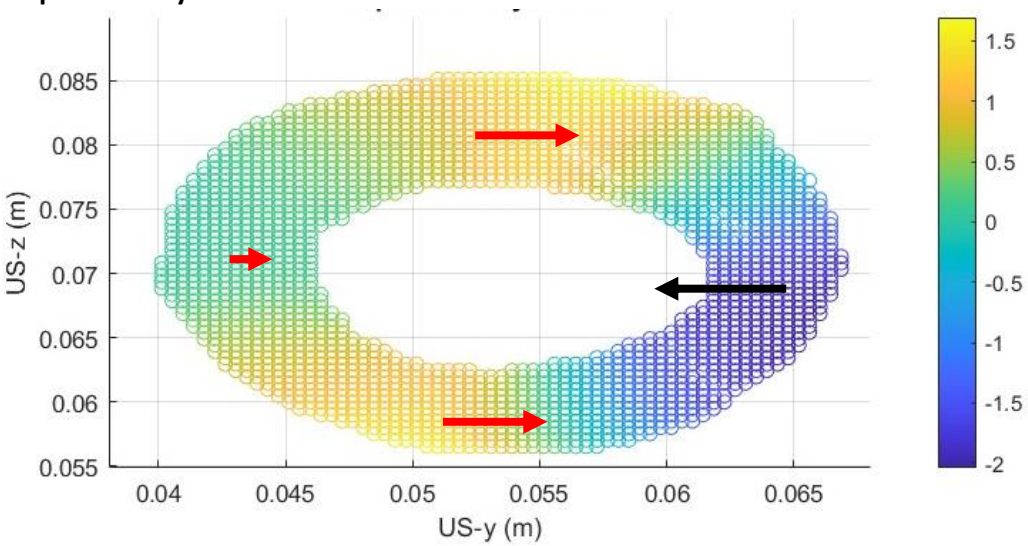

Displacement z-direction

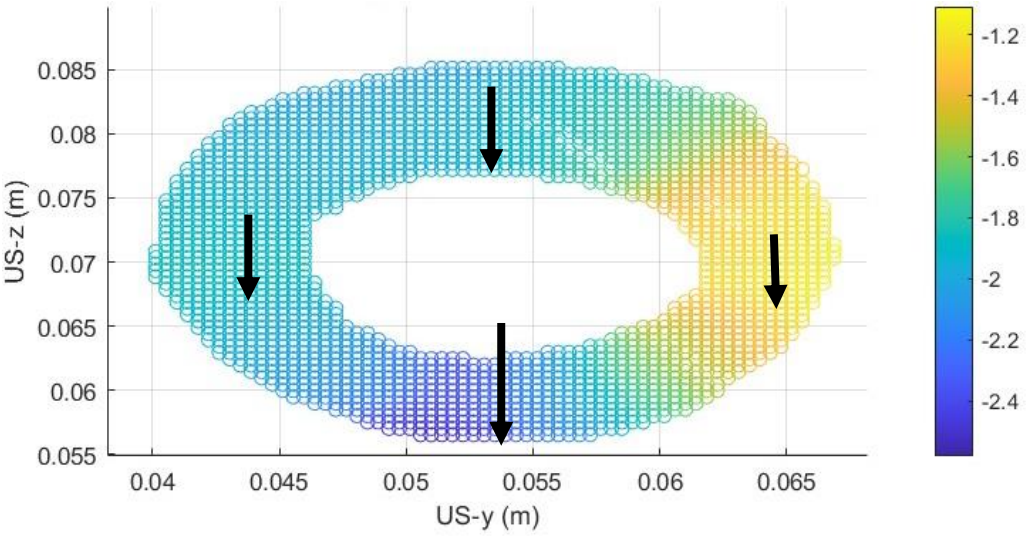

Appendix E: Displacement figures of the patients

Patient 1

Displacement x-direction

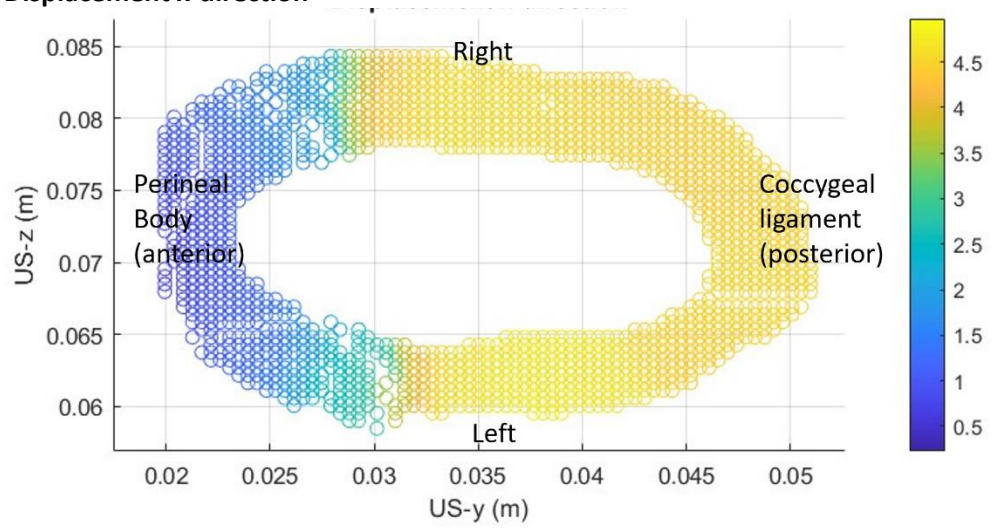

Displacement y-direction

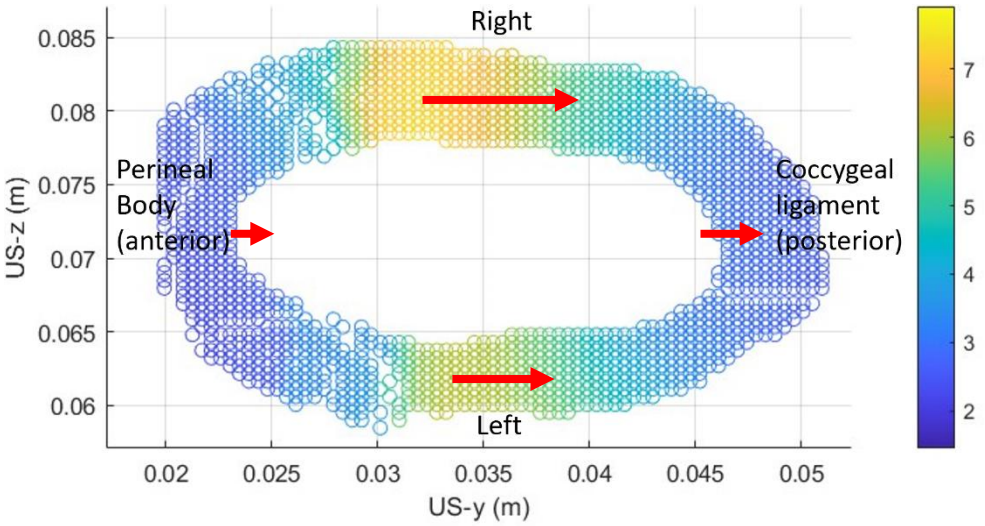

Displacement z-direction

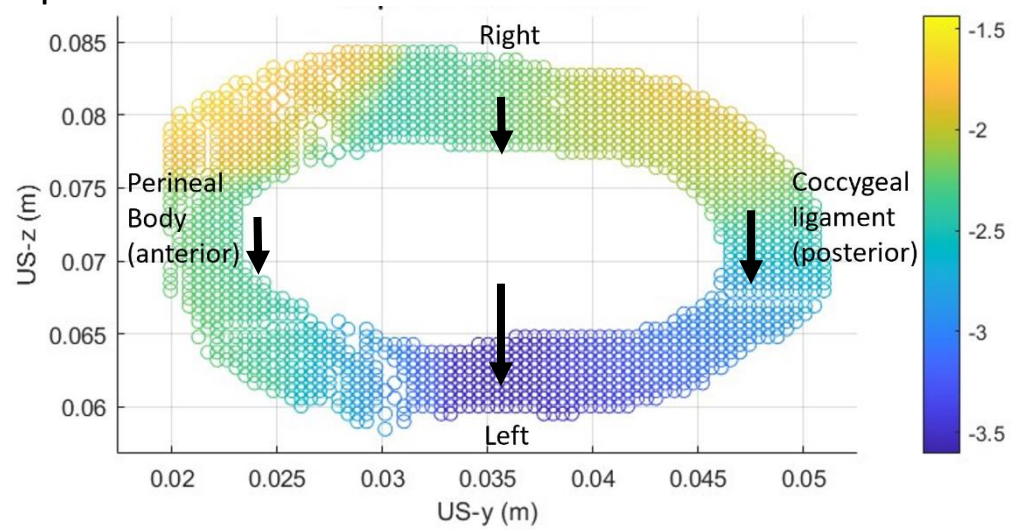

Patient 2

Displacement x-direction

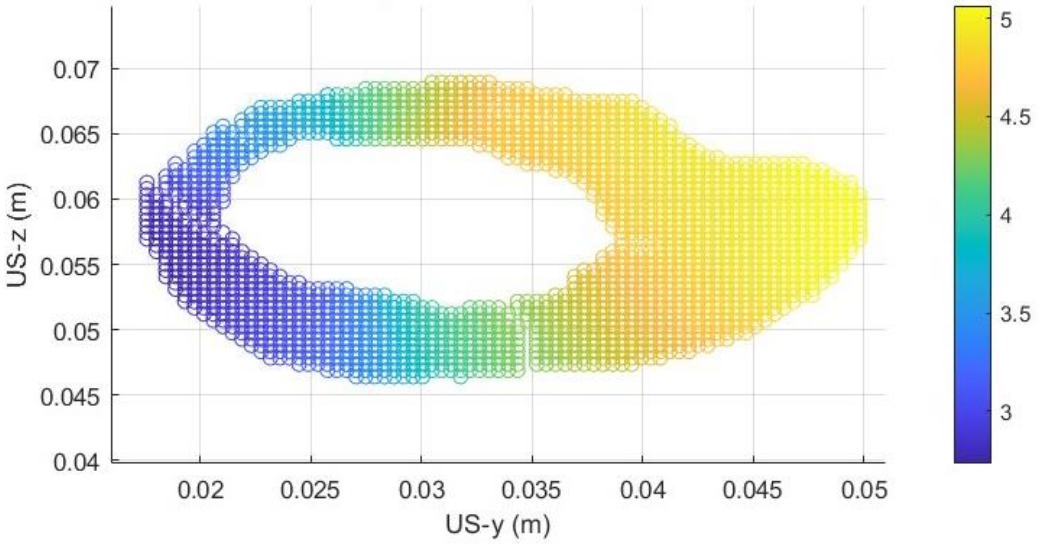

Displacement y-direction

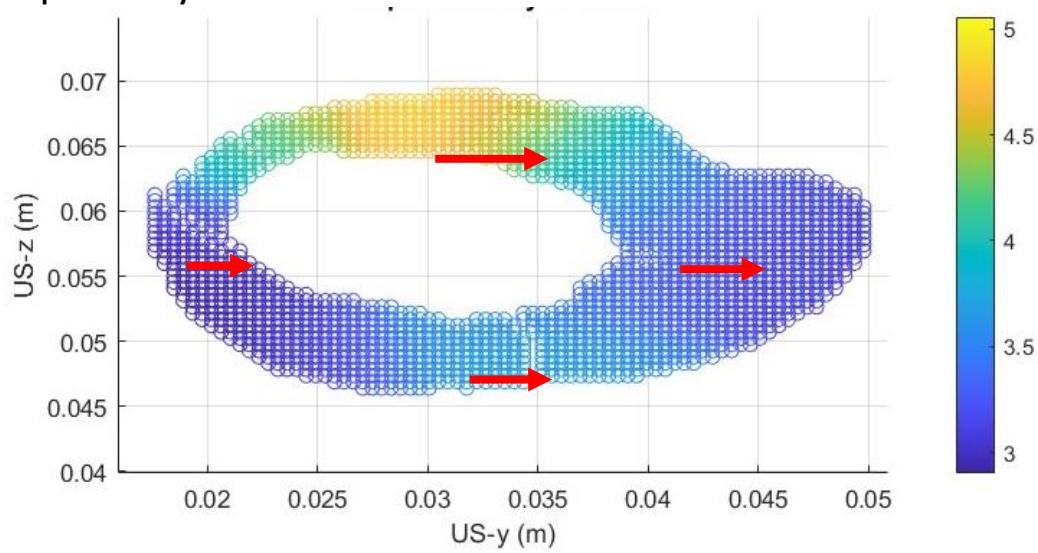

Displacement **z-direction**

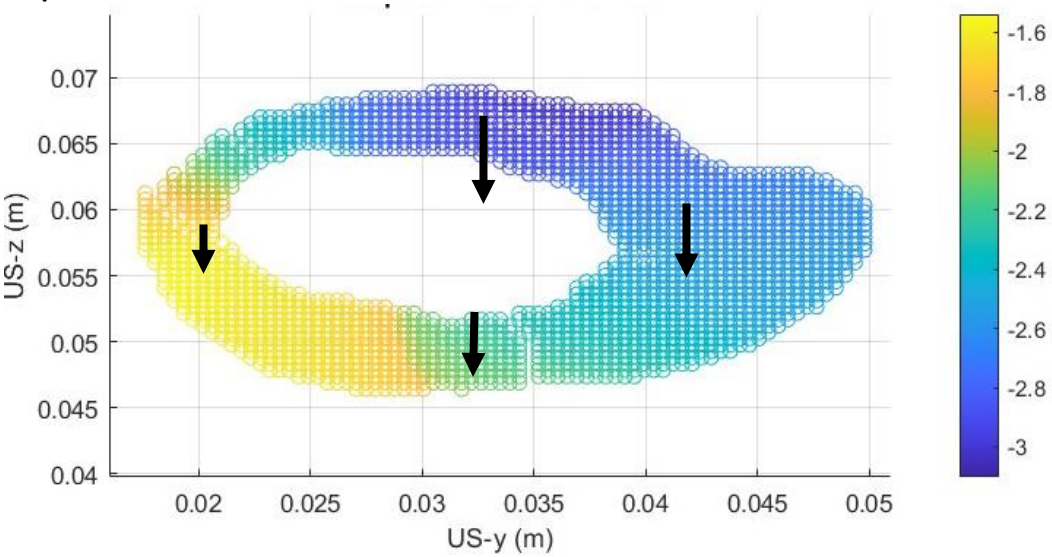

Patient 3

Displacement x-direction

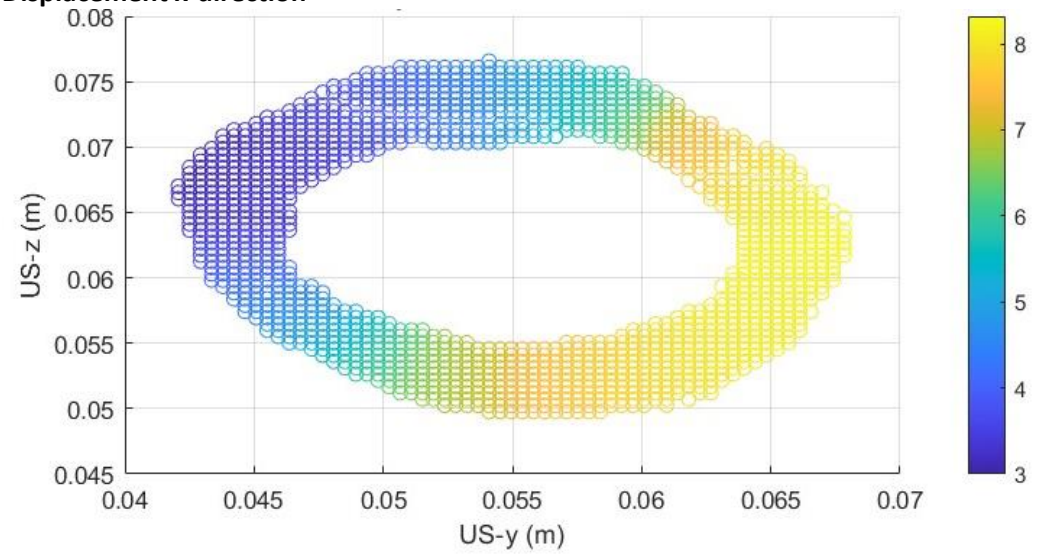

Displacement y-direction

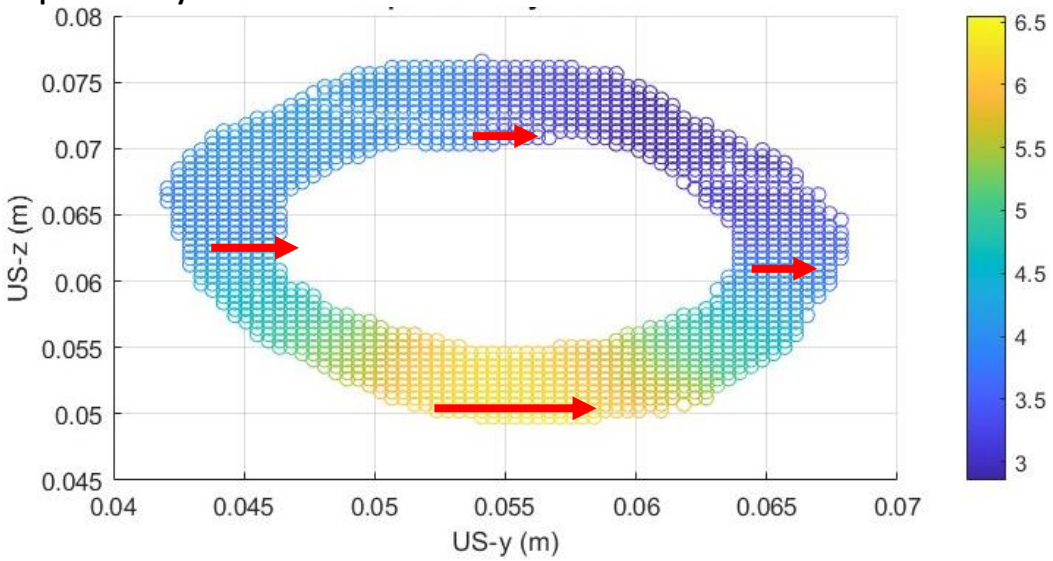

Displacement z-direction

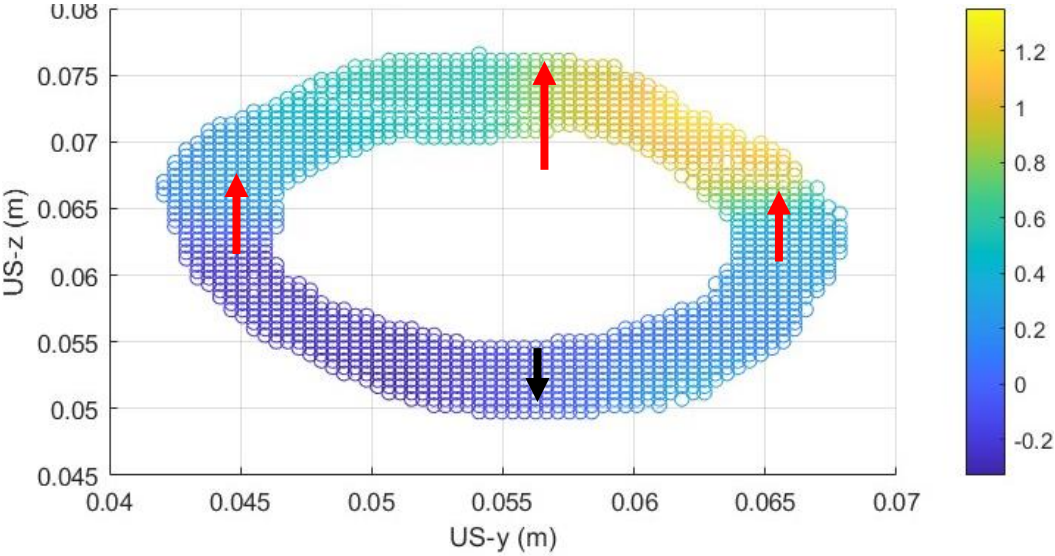

Patient 4

Displacement x-direction

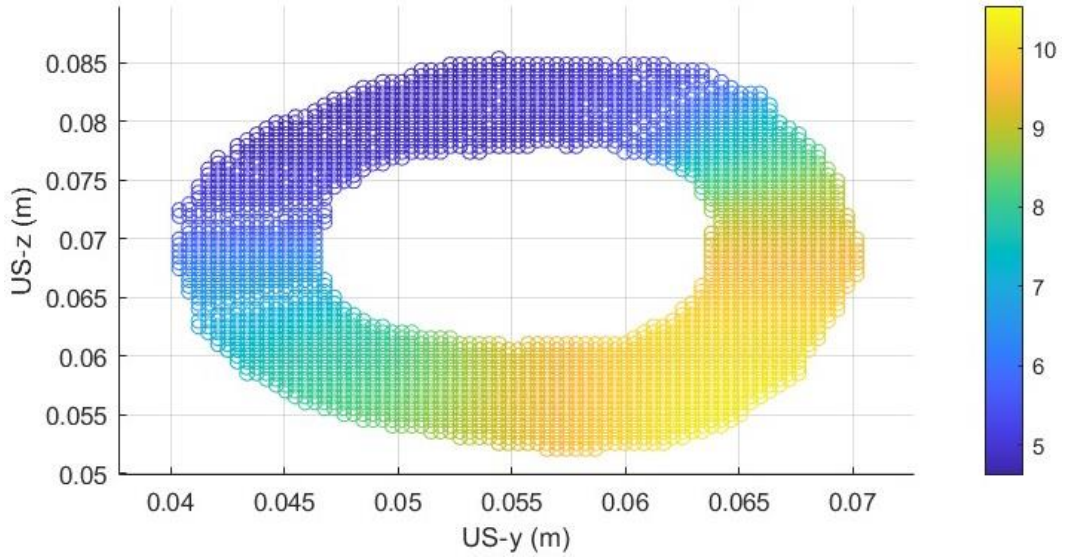

Displacement y-direction

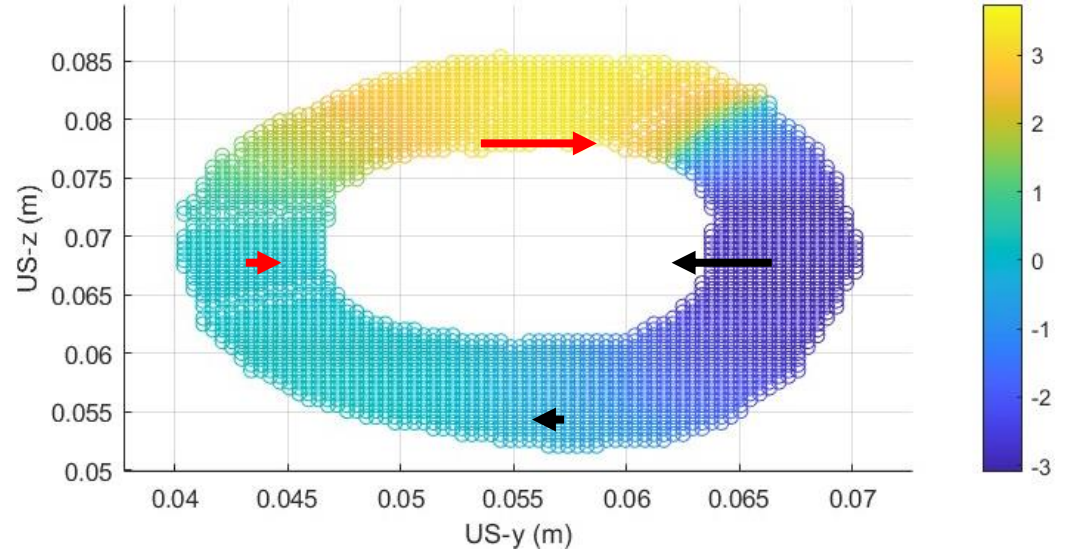

Displacement **z-direction**

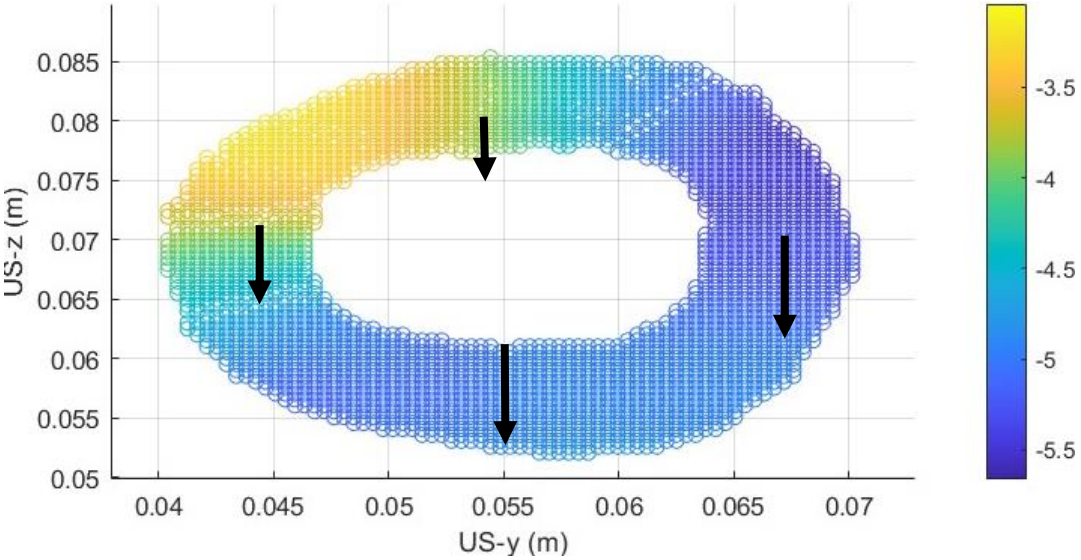

Patient 5

Displacement x-direction

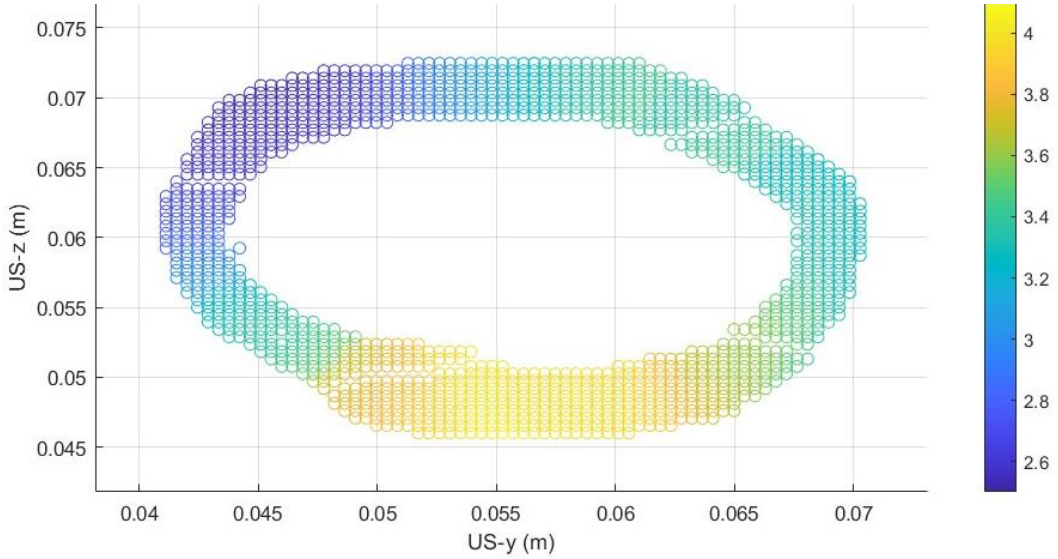

Displacement y-direction

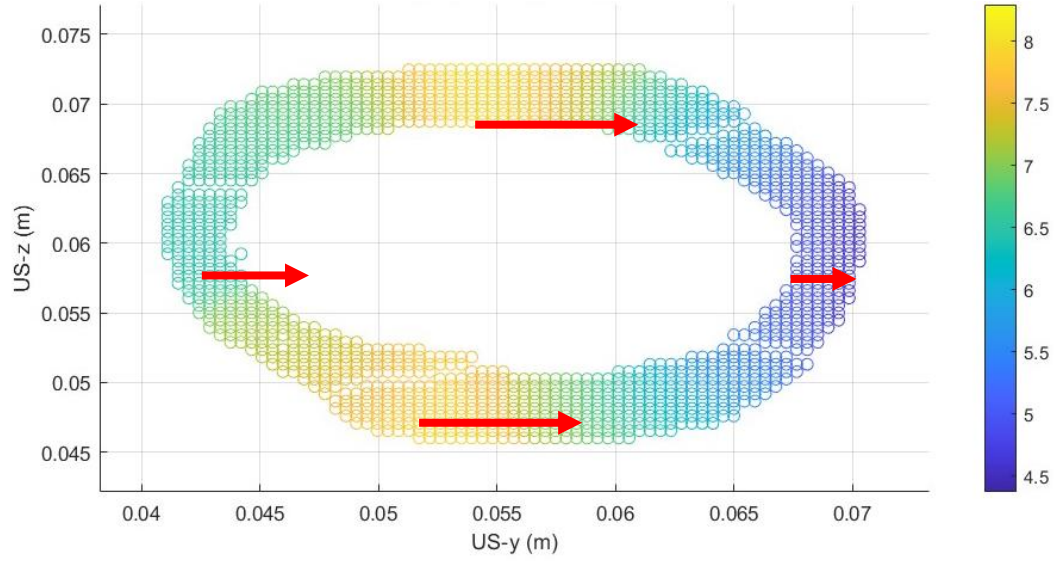

Displacement **z-direction**